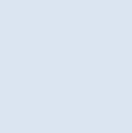


# Modeling of a solar dryer for fruit preservation in developing countries

Juliette Chaignon

Thesis for the degree of Master of Science in  
Engineering  
Division of Heat Transfer  
Department of Energy Sciences  
Faculty of Engineering | Lund University



# Modeling of a solar dryer for fruit preservation in developing countries

Juliette Chaignon

August 2017, Lund

# Acknowledgments

I would like first to thank my supervisor Martin Andersson at the Division of Heat Transfer at Lund University. He has been present to help me whenever I needed it and to give me advice to succeed in both the content and the organization of this thesis work. He gave me new ideas and solutions to improve my model and his knowledge about COMSOL helped me saving a valuable amount of time.

Then, I would like to thank my second supervisor Henrik Davidsson at the Department of Building Design at Lund University. He supervised my work and the regular discussions about it (or other topics) helped me a lot. His knowledge about heat transfer and his common sense have been of great importance in the success of this work.

I would like to thank Etienne Deslandes and Peter Samuelsson and their supervisor Ricardo Bernado. Etienne and Peter built and tested solar dryers and shared the office with me. They made it a nice place to work and the data they provided me with has been of great help. I thank them as well for allowing me to use some of their schematics.

Randi Phinney at the Department of Food Technology at Lund University also deserves a big thank you for all the explanations about the drying process of tangerines juice and for communicating me her motivation about this project.

Finally, I would like to thank the other members of the Solar Food Project, Pia Otte and Lucas Tivana. It was really interesting to get the social science point of view from Pia Otte and Lucas Tivana made the stay in Mozambique easy and very enjoyable.

This project received a grant from SWECO to cover the expenses of a two-weeks field trip to Mozambique which could not have been possible without their support.





# Abstract

About 25,3 % of the Mozambican population is suffering from undernourishment even though a sufficient amount of food and specifically fruits are produced. Post-harvest losses are estimated to 25 % to 40 % and part of the production is not even harvested due to a short season. A solution has to be found to improve fruit preservation and allow the population to consume what is harvested later. Drying fruits is a solution to preserve them. However, juicy fruits are harder to dry than other fruits since they contain more water. One small-scale solution is drying juicy fruits in a specific membrane which allows water vapour to escape from the fruit or the fruit juice to dry. Those membranes have been proven to provide more efficient drying when placed in an airflow or wind. It is possible to couple these membranes with solar dryers technology to control the parameters (temperature, relative humidity, velocity) of such an airflow.

Two types of solar dryers are tested : indirect and direct. Both solar dryers are modeled using a CFD tool (COMSOL Multiphysics) and the modeling work is based on former research to elaborate a mathematical model of the dryers physics. The simulations produced by COMSOL allow to study the influence of several parameters (geometry of the solar dryers, ambient conditions, solar dryers materials) and identify the parameters to consider in order to improve the design of the dryers. The results from the modeling are compared to on-site measurements, in Mozambique, in order to calibrate and validate the models.

**Key words:** solar drying - fruit preservation - indirect solar dryer - direct solar dryer - modeling - CFD



# Contents

<b>Aknowledgments</b>	<b>3</b>
<b>Abstract</b>	<b>5</b>
<b>1 Introduction</b>	<b>1</b>
1.1 Context . . . . .	1
1.1.1 Project background . . . . .	1
1.1.2 Mozambique - location and climate . . . . .	2
1.2 Aims . . . . .	2
1.3 Research questions . . . . .	2
1.4 Guideline . . . . .	4
<b>2 Literature review and background knowledge</b>	<b>5</b>
2.1 Food preservation in Mozambique . . . . .	5
2.1.1 Food insecurity . . . . .	5
2.1.2 Fruit production in Mozambique . . . . .	6
2.1.3 Solar Assisted Pervaporation (SAP) technology . . . . .	7
2.2 Solar Energy in Mozambique . . . . .	9
2.2.1 Limited access to electricity . . . . .	9
2.2.2 Solar thermal potential . . . . .	9
2.3 Solar drying methods . . . . .	10
2.3.1 Solar dryers working principle and classification . . . . .	10
2.3.2 Important parameters of a solar dryer . . . . .	15
2.3.3 Requirements on the quality of the product . . . . .	16

---

<b>3</b>	<b>Method and Theory</b>	<b>17</b>
3.1	Modeling method . . . . .	17
3.1.1	Choice of a simulation software . . . . .	17
3.1.2	Modeling in COMSOL 5.2a and global approach . . . . .	17
3.2	Assumptions . . . . .	18
3.3	Theory . . . . .	22
3.3.1	Heat transfer . . . . .	22
3.3.2	Solar radiation . . . . .	23
3.3.3	Convective heat transfer coefficient . . . . .	24
3.3.4	Radiative heat transfer . . . . .	26
3.3.5	Drying process . . . . .	28
3.4	Models description . . . . .	28
3.4.1	Geometry . . . . .	28
3.4.2	Models description . . . . .	29
3.4.3	Materials . . . . .	29
3.4.4	Ambient data . . . . .	30
3.4.5	Heat transfer module boundary conditions (Model 1) . . . . .	30
3.4.6	Heat transfer module boundary conditions (Model 2) . . . . .	32
3.5	Model validation . . . . .	32
3.5.1	Measurement tools . . . . .	33
3.5.2	Experimental set-up . . . . .	33
3.5.3	Relative error . . . . .	34
<b>4</b>	<b>Results</b>	<b>35</b>
4.1	Tilted passive solar dryer . . . . .	35
4.1.1	Initial values . . . . .	35
4.1.2	Temperature profiles . . . . .	35
4.1.3	Convection coefficient . . . . .	38
4.1.4	Relative humidity . . . . .	39
4.1.5	Energy balance . . . . .	39
4.1.6	Comparison with on-site measurements . . . . .	40
4.2	Parametric studies . . . . .	42

---

4.2.1	Airflow velocity . . . . .	42
4.2.2	External convective heat transfer coefficient . . . . .	42
4.2.3	Internal convective heat transfer coefficient . . . . .	43
4.2.4	Radiative properties . . . . .	44
4.2.5	Insulation thickness . . . . .	47
4.3	Modeling of the active flat solar dryer with SAP-pouches . . . . .	48
4.3.1	Initial values . . . . .	48
4.3.2	Temperature distribution . . . . .	48
4.3.3	Relative humidity . . . . .	49
4.3.4	Comparison with measurements . . . . .	50
<b>5</b>	<b>Discussion</b>	<b>53</b>
5.1	Comparison with measurements . . . . .	53
5.2	Convective coefficient . . . . .	55
5.3	Flow modeling . . . . .	57
5.4	Design optimization . . . . .	57
5.4.1	Solar dryer dimensions . . . . .	57
5.4.2	Materials' radiative properties . . . . .	58
5.4.3	Improving convective effects . . . . .	58
5.4.4	Balance airflow velocity / relative humidity / convection . . . . .	59
<b>6</b>	<b>Appendix</b>	<b>65</b>
A	Friction factor and Nusselt number . . . . .	65



# List of Figures

1.1	Map of Mozambique. The province of Inharrime is located in the south-east part of Mozambique. Source : (Centrale Intelligence Agency 2007), open source . . . . .	3
2.1	Tangerines tree in Inharrime. Personal resource. . . . .	6
2.2	Orange and Mandarine production, losses and export in Mozambique from 2000 to 2014. Data is obtained with permission from Food and Agriculture Organization of the United Nations. © (Food Agricultural Organization of the United Nations 2014b). . . . .	7
2.3	SAP process - Source : (Phinney and Tivana 2016) . . . . .	8
2.4	Average solar irradiation in Inharrime and Lund from 1984 to 2005 - Source : (Bengtsson, G. and Döhlen, V. 2016) . . . . .	10
2.5	Annual averages of solar irradiation ( $kWh/m^2/day$ ) in Tanzania and Mozambique - Source : (Hammar 2011) . . . . .	11
2.6	Design of a direct solar dryer - Courtesy of Etienne Deslandes and Peter Samuelsson . . . . .	12
2.7	Working principle of an indirect solar dryer - Courtesy of Etienne Deslandes and Peter Samuelsson . . . . .	13
2.8	Design of a passive hybrid solar dryer -Source : (Ekechukwu, O.V. and Norton, B. 1999) . . . . .	14
3.1	Schematics of the solar dryers modeled in COMSOL - Images courtesy of Etienne Deslandes and Peter Samuelsson . . . . .	20
3.2	Exploded view of the solar dryers - Image courtesy of Etienne Deslandes and Peter Samuelsson . . . . .	21
3.3	Schematics of the heat transfer exchange in a solar dryer cross-section . . .	22

3.4	Pictures of experimental set-up and measurement tools . . . . .	33
3.5	Schematics of the outlet of the solar dryer and identified points of measurements . . . . .	34
4.1	Reference lines used to plot the temperature profiles . . . . .	36
4.2	Zoom on the reference lines used to plot the temperature profiles . . . . .	37
4.3	Temperature profiles - Tilted passive solar dryer . . . . .	38
4.4	Graph : Internal convective heat transfer coefficient on the absorber depending on the velocity - Tilted passive solar dryer model . . . . .	43
4.5	Graph - Internal convective coefficient on the absorber plate - Tilted passive solar dryer model . . . . .	44
4.6	Graph - Outlet air temperature and relative humidity depending on the plastic value for transparency . . . . .	45
4.7	Graph - Outlet air and absorber temperature depending on the absorber emissivity . . . . .	46
4.8	Graph - Evolution of the outlet air temperature depending on the insulation thickness . . . . .	47
4.9	Relative humidity distribution around the active solar dryer - Model 2 . . .	49
4.10	Relative humidity distribution inside the active solar dryer - Model 2 . . .	50
5.1	Schematics of a bump showing the height of one bump of the metal sheet. This metal sheet is modeled as a flat sheet, which thickness is half of the height of a bump. . . . .	55
6.1	Graph : Friction factor for different values of airflow velocity - comparison of two formulas . . . . .	66
6.2	Graph : Nusselt number for different values of airflow velocity - comparison of two formulas . . . . .	66



# List of Tables

3.1	Materials' properties . . . . .	29
3.2	Absorber heat transfer . . . . .	30
3.3	Plastic sheet heat transfer . . . . .	31
3.4	Sides and bottom heat transfer . . . . .	32
4.1	Input data for tilted passive solar dryer in Inharrime . . . . .	36
4.2	Temperatures of the different elements at the outlet of the collector . . . . .	37
4.3	Convective heat transfer coefficient . . . . .	38
4.4	Energy balance of the tilted passive solar dryer on half on the collector . . . . .	40
4.5	Comparison between model 1 and actual measurements for temperature . . . . .	41
4.6	Temperatures of the different elements on the front side of the collector . . . . .	48
4.7	Comparison between model 1 and actual measurements for temperature . . . . .	51



# Nomenclature

$\tau$	Transmittance	-
$\alpha$	Absorptance	-
$\nabla$	Nabla operator	-
$\rho$	Density	kg/m <sup>3</sup>
$\theta$	Solar dryer inclination angle	°
$A_{bags}$	Surface of a bag	m <sup>2</sup>
$abs$	Absorber	
$C_p$	Specific heat at constant pressure	J/kg · K
$E_{vap}$	Energy required from a solar assisted pervaporation pouch for water evaporation	W
$F_{amb}$	Ambient view factor	-
$g$	Gravitational constant	m/s <sup>3</sup>
$G_e$	Effective solar radiation	W/m <sup>2</sup>
$G_m$	Mutual irradiation	W/m <sup>2</sup>
$h_{conv,in}$	Internal convective heat transfer coefficient	W/m <sup>2</sup> ·K
$h_{conv,out}$	External convective heat transfer coefficient	W/m <sup>2</sup> · K
$k$	Thermal conductivity	W/m
$m_{vap}$	Water massflow evaporated	kg/s
$Nu$	Nusselt number	-

$p$	Plastic sheet	
$Q$	Heat sources	W/m <sup>3</sup>
$q$	Heat flux by conduction	W/m <sup>2</sup>
$R$	Reflection coefficient	-
$Ra_L$	Rayleigh number	-
$T$	Absolute temperature	K
$T_{abs}$	Temperature of the absorber	K
$T_{air}$	Temperature of the air circulating in the solar dryer	K
$T_{amb}$	Temperature of the ambient air	K
$T_{plast}$	Temperature of the plastic sheet	K
$T_{sky}$	Temperature of the sky	K
$u$	Velocity vector	m/s
$u_{bags}$	Airflow velocity around the bags	m/s

# Chapter 1

## Introduction

*This chapter gives a background on the project and states the aims of this work. Then, research questions and guideline are given.*

### 1.1 Context

#### 1.1.1 Project background

This degree project is carried out at the department of Energy Sciences at Lund University. It is part of a collaborative work involving the following institutions : the department of Energy and Building Design and the department of Food Technology, Engineering and Nutrition in Lund, the Centre for Rural Research in Trondheim and Eduardo Mondlane University in Mozambique. This research project focuses on combining solar drying technology with innovative membrane bags using solar assisted pervaporation (details in Section 2.1.3) in order to facilitate the drying of juicy fruits in Mozambique. The combination of these two technologies aims to ensure the preservation of different types of fruits while increasing the quality of the dried product.

Previous research have been conducted through a Master thesis in the Department of Energy and Building Design in Lund to evaluate the interest of combining the membrane bags and a Solar Driven Convective Dryer. Then, two other degree projects dwelt respectively on building a solar dryer and measuring its performance in Mozambique and on elaborating a mathematical and theoretical model of the aforementioned solar dryer. The results called for further research on modeling and designing a new solar dryer in order to increase its performance.

This project is linked to a larger research project, The *Solar Food Project*, which aims

to reduce food waste and offer more economic security to small-scale farmers in rural areas of Mozambique. The implementation of this project in Mozambique is motivated by the historic collaboration between the department of Food Technology in Lund and Eduardo Mondlane University in Mozambique.

The aim to combine solar drying technology, which is a common and already well-known way of preserving fruits, with newly developed membrane bags makes this project singular. The field tests will be conducted in the province of Inharrime in Mozambique.

### 1.1.2 Mozambique - location and climate

Mozambique is a country located in the Southeast of Africa. It is crossed by the Capricorn cancer and the climate there is tropical. The northern part and the coastal part are considered humid tropical while the southern part, where the province of Inharrime is located (Fig.1.1), has a dry tropical climate (Centrale Intelligence Agency 2007).

## 1.2 Aims

The aims of this thesis are to :

- create a model with a CFD tool from the already available mathematical model
- compare the models with measurements done on-site
- suggest an optimized design of a solar dryer after analyzing the results of the calculations done with the model created on COMSOL Multiphysics

## 1.3 Research questions

This work aims to answer the following research questions :

- How to adapt the given mathematical model to a CFD tool ?
- Is the model consistent with measurements ?
- How to optimize the solar dryer based on the implementation of the mathematical model on a CFD tool ?



Figure 1.1: Map of Mozambique. The province of Inharrime is located in the southerneast part of Mozambique. Source : (Centrale Intelligence Agency 2007), open source

## 1.4 Guideline

After giving background information about fruit preservation, solar energy and solar drying in Mozambique, a section will be dedicated to explaining the modeling approach and the theory needed to build the models. Then, the results of the modeling work will be presented. Finally, these results will be discussed and some design optimization will be proposed.



# Chapter 2

## Literature review and background knowledge

*This chapter aims to give background knowledge regarding the need for fruit preservation in Mozambique, the solar assisted pervaporation technology, solar energy in Mozambique and solar dryers.*

### 2.1 Food preservation in Mozambique

#### 2.1.1 Food insecurity

Mozambique is a developing country which presents a high rate of undernourished people. Around 6,9 million inhabitants are undernourished which represents 25,3 % of the total population in Mozambique (Food Agricultural Organization of the United Nations 2016). The situation is even more concerning for children since 43 % of the children under 5 years old suffer from chronic malnutrition and 6 % are considered as sharply malnourished (Instituto Nacional de Estatística 2012).

This problem can be explained by the fact that although an acceptable amount of food is grown, a significant part is not consumed due to harvest losses or spoilage before it can be consumed. Post-harvest losses are estimated between 25 % and 40 % in Mozambique and a large part of the fruit production is not even harvested due to a short season (Phinney, R., Rayner, M., Sjöholm, I., Tivana, L. and Dejmek, P. 2015).

A solution to cope with this issue is to provide a fruit processing technology to safely and cost-efficiently preserve fruits when they can be harvested in order to consume them later. Large-scale solutions such as canning or aseptic processing are economic but they

also require a considerable amount of resources (clean water, energy, transport facilities) which are not necessarily available in developing countries like Mozambique (Andersson 2016).

### 2.1.2 Fruit production in Mozambique

Thanks to a favorable climate and a high amount of available arable land, fruits are easily grown in Mozambique. This country produces top quality bananas, citrus, avocados, mangoes, litchis, pinapples, papaya, passion fruit, strawberry and guava. In particular, citrus fruits such as lemons, oranges, tangerines and grapefruits are produced between March and September (the peak season is variable depending on the fruit type) (TechnoServe 2002).



Figure 2.1: Tangerines tree in Inharrime. Personal resource.

This thesis work focuses on tangerines cultivated in Inharrime (Fig. 2.1) because these are the fruits used during field tests. In 2014, about 426 tons of tangerines were produced in Mozambique (Food Agricultural Organization of the United Nations 2014a). Figure 2.2 shows the orange and mandarine production, losses and export in Mozambique for the past 14 years. The data for tangerines is not accessible, however it is possible to assume that the trend is the same, with losses higher than export (Food Agricultural Organization of the United Nations 2014b).

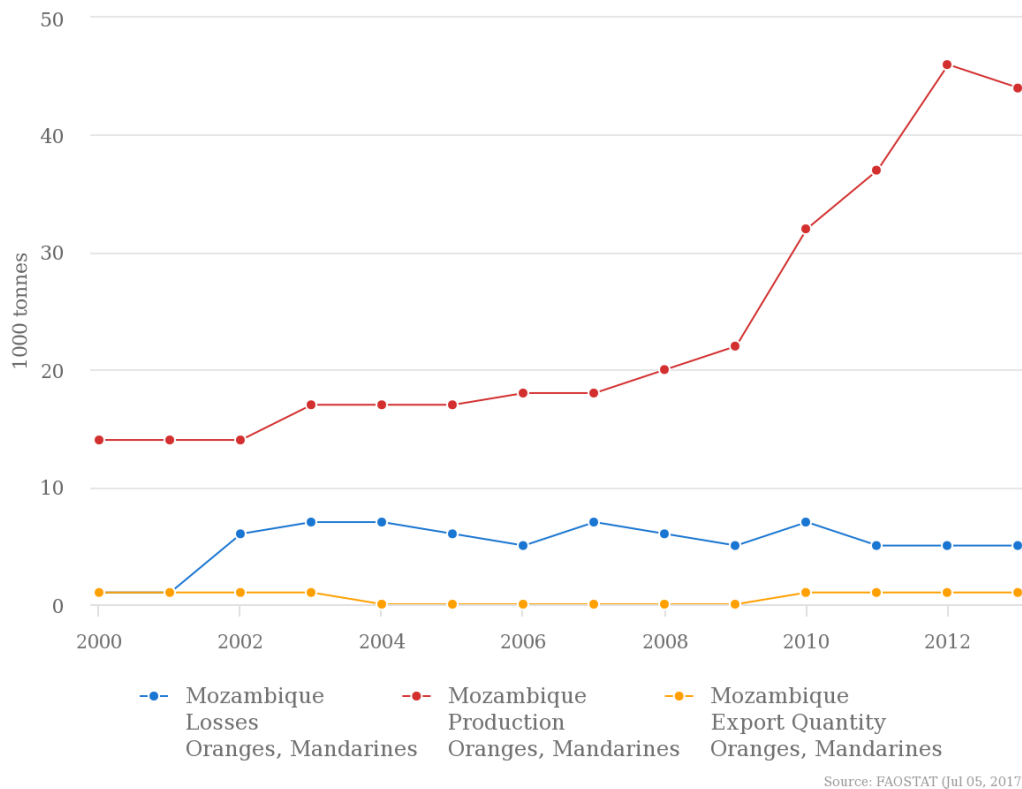


Figure 2.2: Orange and Mandarin production, losses and export in Mozambique from 2000 to 2014. Data is obtained with permission from Food and Agriculture Organization of the United Nations. © (Food Agricultural Organization of the United Nations 2014b).

### 2.1.3 Solar Assisted Pervaporation (SAP) technology

A small-scale solution to preserve fruit is Solar Assisted Pervaporation, a technology developed by the Food Technology Department at Lund University. Pervaporation is the transport of a chemical specie from one side of a nonporous semipermeable membrane to the other and occurs by diffusion (Phinney, R., Rayner, M., Sjöholm, I., Tivana, L. and Dejmek, P. 2015). This technology allows to dry fruits by using a semipermeable membrane which allows water vapour to escape the bag and prevents liquid water from entering it (Fig. 2.3).

The criteria used to determine if a product has been dried enough and is suitable for conservation at room temperature is the water activity level  $a_w$ . The water activity corresponds to the ratio between the vapor pressure of the food ( $P_w$ ) to the vapor pressure of water at the same temperature and pressure ( $P_{ws}$ ) (Phinney, R., Rayner, M., Sjöholm, I., Tivana, L. and Dejmek, P. 2015) and can also be expressed as the equilibrium relative

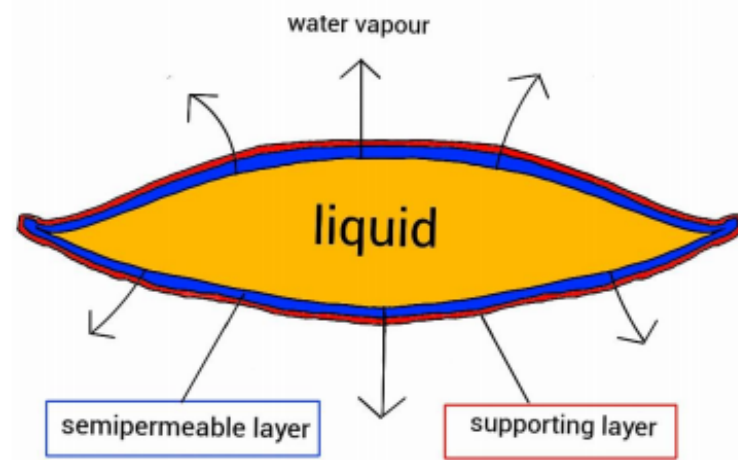


Figure 2.3: SAP process - Source : (Phinney and Tivana 2016)

humidity of the product divided by 100 (Singh, P. and Heldman, D.R. 2013). This relation is found in equation (2.1).

$$a_w = \frac{P_w}{P_{ws}} = \frac{RH}{100} \quad (2.1)$$

Water activity aims to consider the water which is available for microbial growth in the product and is different from the water content of the product. In order to prevent bacterial growth in the product the water activity has to be lower than 0,7. The food is then considered storage stable at ambient temperature since it is impossible for yeasts, bacteria or molds to grow (Phinney, R., Rayner, M., Sjöholm, I., Tivana, L. and Dejmek, P. 2015). A low pH (as in acid fruits) also participates in limiting bacterial growth.

The membrane bags are re-usable and can be used to dry either fruit juice, fruit purée or even fruit pieces. The drying performance of SAP membrane bags were observed for mango purée, apple purée and lemon juice. The conclusions made in (Phinney, R., Rayner, M., Sjöholm, I., Tivana, L. and Dejmek, P. 2015) are that :

- The drying process using SAP-pouches allows to reach water activities below 0,7. For instance, mango purée water activity went from 1,0 to 0,48 after 45 hours of drying.
- Ambient relative humidity is a key parameter in the drying process and is related to the temperature. A lower relative humidity will provide a higher evaporation rate of the product inside the pouch.

- Ambient wind velocity that is the velocity of the air flow around the pouch decreases the drying time.

Given these conclusions, combining SAP membrane bags and solar thermal technology could be a way of providing heated air thus decreasing the ambient relative humidity around the membrane bag and creating a convective air movement around the bags. One aim of this study is to compare the performance of the drying process with natural and forced convection.

## 2.2 Solar Energy in Mozambique

### 2.2.1 Limited access to electricity

The electrification in Mozambique is very limited with only 18 % of the population being reached by the national grid. On top of this, there are high losses (about 25 %) due to transmission and distribution (Amin 2013). Thus, solar thermal energy is an alternative to heat air and favours the drying process of the product inside the membrane bags without requiring electricity or needing an amount of electricity provided through a self-sufficient system (such as photovoltaic cells for instance).

### 2.2.2 Solar thermal potential

Solar thermal technology uses solar radiation as a source of energy. As Mozambique is a tropical country in the southern hemisphere, it receives a consequent amount of solar radiation. Figure 2.5 shows the annual averages of insolation in Mozambique and Tanzania (given in kWh/m<sup>2</sup>/day) taken from ground measurements and interpolation found in Hammar (2011). The average amount of solar radiation varies depending on the geographical location in the country. However, the annual average solar radiation is estimated to be 5,2, kWh/m<sup>2</sup>/day and varies from 4 kWh/m<sup>2</sup>/day to 7 kWh/m<sup>2</sup>/day across the country (Amin 2013).

It is possible to compare the solar irradiation in the province of Inharrime (Mozambique) to Lund (Sweden) taken as a reference. The months of March, April and May occur during fall and winter in Mozambique since the country is located in the southern hemisphere. This period has to be compared with the months of September, October and November. Figure 2.4 shows that Lund receives about half of the solar irradiation that is received in the province of Inharrime. Thus Mozambique receives an interesting amount of solar

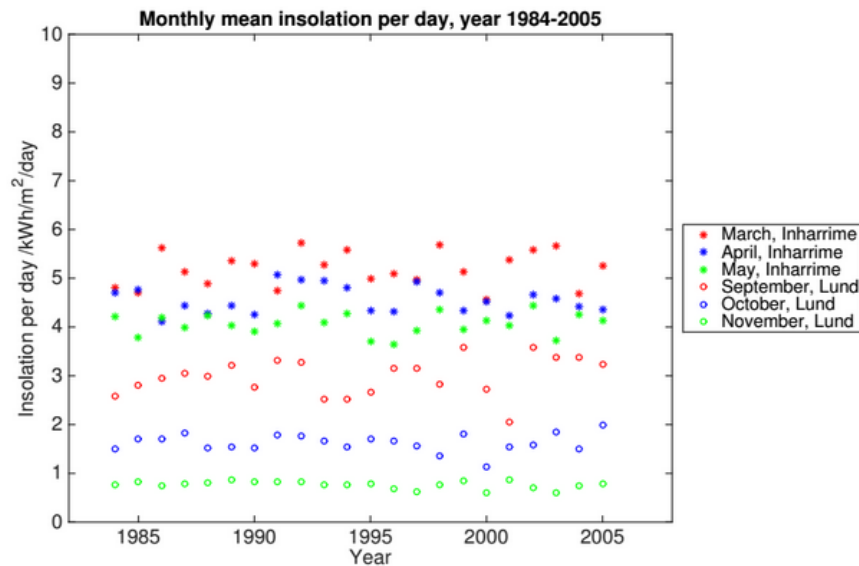


Figure 2.4: Average solar irradiation in Inharrime and Lund from 1984 to 2005 - Source : (Bengtsson, G. and Döhlen, V. 2016)

radiation and it confirms the potential for the use of thermal solar energy in this location to dry fruits.

## 2.3 Solar drying methods

The point in using a solar dryer is to provide more heat than the ambient air could provide to SAP membrane bags (Ekechukwu, O.V. and Norton, B. 1999). The two main technologies regarding solar drying are respectively active and passive solar dryers. Among these two categories it is possible to use indirect, direct or mixed solar drying systems.

### 2.3.1 Solar dryers working principle and classification

**Active and passive solar dryer** A passive solar dryer only relies on a natural convective heat transfer, the heated fluid's flow being created by buoyancy force. One advantage of this type of solar dryer is that it does not require any extra source of energy. On the opposite, in an active solar dryer, the heated fluid is forced to circulate by a fan, a blower or any equivalent element. It requires an additional source of energy (Ekechukwu, O.V. and Norton, B. 1999).

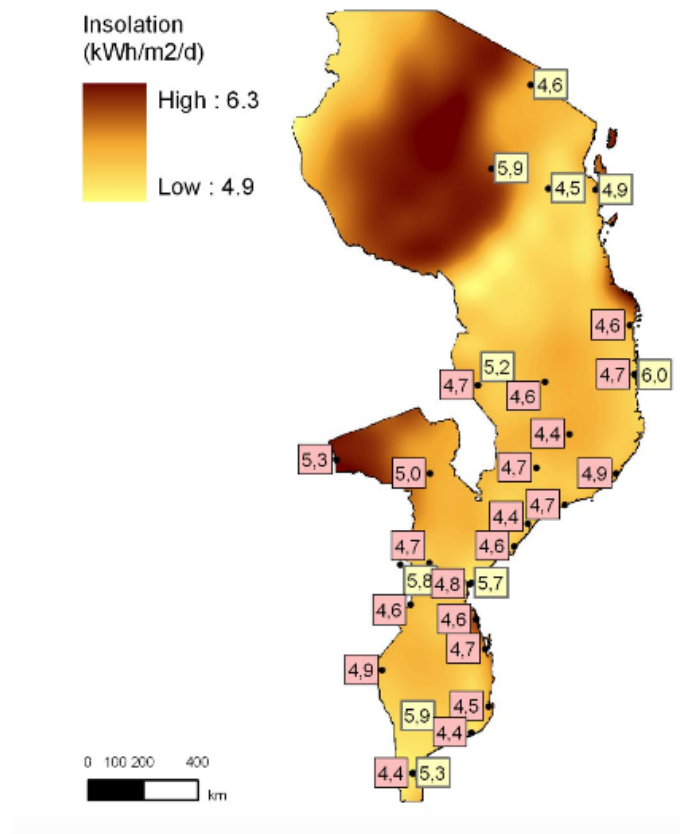


Figure 2.5: Annual averages of solar irradiation ( $kWh/m^2/day$ ) in Tanzania and Mozambique - Source : (Hammar 2011)

**Direct solar drying** In a direct solar dryer, the products are directly exposed to the solar radiations. As shown on Figure 2.6, a solution is to put the products under a transparent cover such as glass or plastic. The advantage of such a method is its simplicity and low price since material and maintenance require low investment.

A direct solar dryer usually has a drying chamber consisting in an insulated box covered by a transparent cover (glass or plastic) and having air holes to allow air to enter and exit the chamber. The solar radiation arrives on the glass cover and heats up the air which circulates either naturally (passive solar dryer) or by wind pressure using external sources (active solar dryer) or both (Sharma, A., Chen, C.R. and Vu Lan, N. 2009). Part of the solar radiation is reflected back by the transparent cover to the atmosphere whereas the remaining part is transmitted inside the dryer chamber. Part of the transmitted radiation is reflected from the product surface but the rest is absorbed by it and thus the product temperature increases enabling to reduce its moisture content by evaporation (Kumar, M., Sansaniwal, S.K. and Khatak, P. 2016).

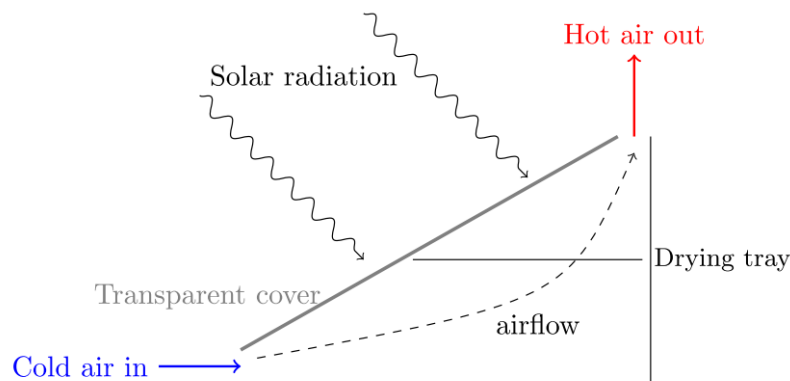


Figure 2.6: Design of a direct solar dryer - Courtesy of Etienne Deslandes and Peter Samuelsson

However, a direct solar dryer presents the following limitations (Sharma, A., Chen, C.R. and Vu Lan, N. 2009) :

- its small-capacity limits it to a small-scale use
- the direct exposure to solar radiation can cause chemical reactions such as discoloration of crops
- while drying the moisture condensates on the glass and can affect its transmittivity
- if the temperature of the product is not high enough, the moisture removal can be difficult



- the use of selective coatings for the absorber plate<sup>1</sup> is limited

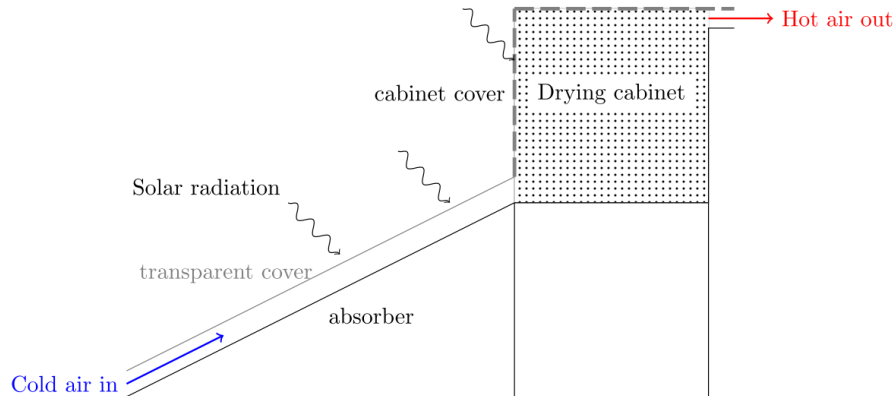


Figure 2.7: Working principle of an indirect solar dryer - Courtesy of Etienne Deslandes and Peter Samuelsson

**Indirect solar drying** The indirect solar drying working principle relies on the use of solar radiation by a solar collector to heat air, and the product to be dried is not directly exposed to solar radiation so it is possible to avoid the discoloration of the product (Sharma, A., Chen, C.R. and Vu Lan, N. 2009) and vitamins degradation. These solar dryers include the following components (Ekechukwu, O.V. and Norton, B. 1999) :

- an air-heating solar collector
- a drying chamber
- eventually a chimney

Air enters in the collector where it is heated by the solar radiation. The solar collector unit allows to provide higher temperatures in the drying chamber and the control of the air flow rates (Kumar, M., Sansaniwal, S.K. and Khatak, P. 2016). It is then possible to design a solar collector to obtain a given outlet temperature of the air. The air heated by the solar collector part can then circulate around the products to be dried in the drying chamber as shown on Figure 2.7. Since the air is at a higher temperature than the product, there is a heat transfer by convection which provides moisture evaporation and thus drying. The convection providing heat transfer in the drying chamber can be either natural (due to upthrust force or wind pressure) in passive indirect solar dryer or forced (thanks to fans or pumps which enhance air circulation) in an active indirect solar dryer (Sharma, A., Chen, C.R. and Vu Lan, N. 2009).

<sup>1</sup>The role of the absorber in a solar dryer will be detailed later in Section 3

**Mixed solar drying** A mixed solar dryer working principle aims to use solar radiation for both direct heating of the product and preheating of air thanks to a spare energy source such as solar energy or biomass heater (Kumar, M., Sansaniwal, S.K. and Khatak, P. 2016). Figure 2.8 presents an example of an hybrid passive solar dryer. This model is very similar to a classic passive indirect solar dryer except that the drying chamber's walls are made of glass so the direct solar radiation can impinge the product to be dried (Ekechukwu, O.V. and Norton, B. 1999).

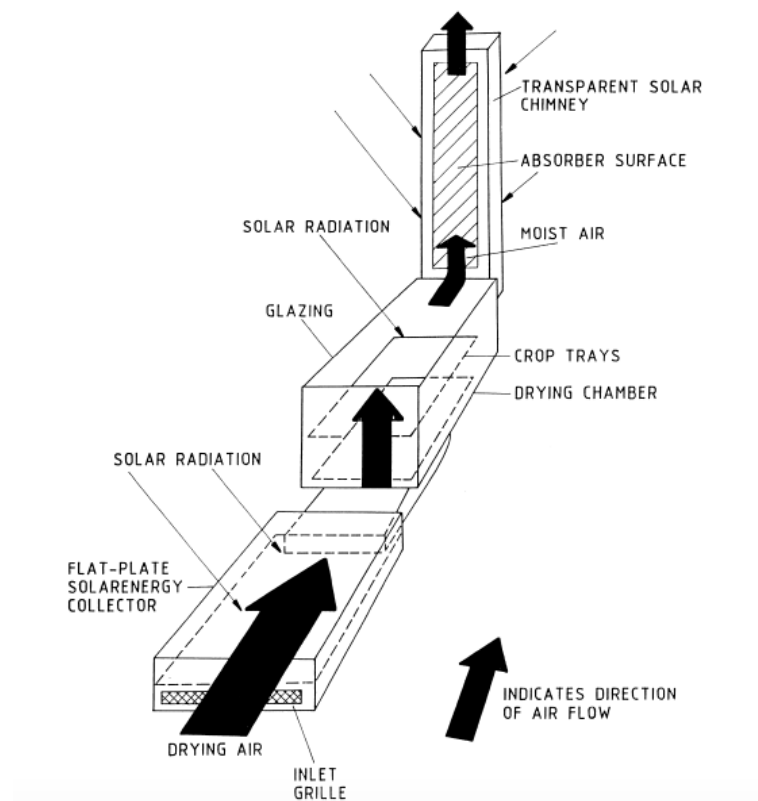


Figure 2.8: Design of a passive hybrid solar dryer -Source : (Ekechukwu, O.V. and Norton, B. 1999)

Several studies compared the performance of a mixed solar dryer with an indirect or direct solar dryer. Hybrid solar dryers have been found to provide an increased drying rate without affecting the quality of the product (Kumar, M., Sansaniwal, S.K. and Khatak, P. 2016). However, these systems are more complex and less common (Sharma, A., Chen, C.R. and Vu Lan, N. 2009).

### 2.3.2 Important parameters of a solar dryer

A major point to consider when it comes to design and optimize a solar dryer in Mozambique is the fact that the access to water and electricity is highly limited there, as mentioned above (see Section 2.2). For this reason, a passive solar dryer seems more appropriate in rural areas than an active solar dryer that would require a motorised fan (Ekechukwu, O.V. and Norton, B. 1999). Previous studies about fruit drying in membrane pouches first showed that indirect solar drying was preferable to avoid damaging effects on nutrients or chemicals reactions altering the product. However, more recent results suggest that direct solar radiation is suitable for membrane pouches (Phinney and Tivana 2016). In order to design and optimize a solar dryer, two main parameters can impact its performance.

#### Temperature

Temperature is one of the most important parameters along with air velocity and relative air humidity as found in the conclusions of (Phinney, R., Rayner, M., Sjöholm, I., Tivana, L. and Dejmek, P. 2015) aforementioned in Section 2.1.3. A higher temperature in the drying chamber provides a higher drying rate for two main reasons (Augustus, L., Kumar, S. and Bhattacharya, S.C. 2002) :

- A higher temperature of the drying air increases its ability to retain humidity.
- A higher temperature of the drying air allows to heat the product and thus to increase its vapor pressure forcing the moisture to go on the surface faster.

Temperature has a major role in the performance of a drying process because the driving force for this process is the difference between the vapor pressure of the liquid water surface of the product and the vapor pressure in the air around the surface of the product (Singh, P. and Heldman, D.R. 2013). Thus, increasing the temperature of the air in the drying chamber triggers a drop in the partial pressure of moisture in the air and then increases the vapor pressure difference between the product and its surrounding air. The diffusion of water from the product to the air will thus be increased and it will result in a higher drying rate (Bengtsson, G. and Döhlen, V. 2016). In the particular case of membrane pouches, a higher partial pressure difference provides a higher pervaporation rate through the membrane of SAP-pouches (Kumar 2010).

### **Airflow**

The airflow velocity importance in the solar dryer can be discussed. According to (Kumar, M., Sansaniwal, S.K. and Khatak, P. 2016), it is possible to reduce the drying time from 14,89 % to 37,66 % compared to a natural solar drying with increasing air velocity in the solar dryer. But this result applies for crops (i.e. rice, corn, potatoes) and air velocity has a small influence on the drying process of most of vegetables and fruits (Onwunde, D. I., Norhashila, H. , Rimfiel, B.J., Nazmi, M.N. and Khalina, A. 2010). The impact of an high velocity of the airflow in the drying chamber is limited and the fluctuations of the airflow velocities are small in the drying chamber and thus can be neglected (VijayaVinkataRaman, S., Iniyan, S. and Goic, R. 2012).

### **2.3.3 Requirements on the quality of the product**

It is possible to give criteria in order to assess food safety and a minimum level of quality for the dried product. A temperature interval required in the drying chamber has been set by the Department of Food Technology at Lund University. A minimum temperature of 50°C is required in order to avoid bacterial growth. The temperature also has to stay below 65°C to avoid the degradation of acid ascorbic (Vitamin C) (Bengtsson, G. and Döhlen, V. 2016) contained in the fruits which are found in Mozambique (tangerines, mandarins).

# Chapter 3

## Method and Theory

*This chapter aims to present the modeling method with COMSOL software and the underlying theory.*

### 3.1 Modeling method

#### 3.1.1 Choice of a simulation software

COMSOL Multiphysics is a physics-based modeling and simulation software using finite elements to run calculations.

The choice of COMSOL as a simulation software is justified by several reasons. The conclusions in (Olsson 2016) highly recommend to use a CFD tool to carry out the modeling work. Actually, COMSOL is a well-known program for heat transfer and fluid dynamics and it provides information on heat transfer profiles and fluid behaviour inside the solar dryer (Singh Chauhan, P., Kumar, A. and Tekasakul, P. 2015). Singh et al. (2015) also precises that COMSOL Multiphysics is user-friendly and easier to learn compared with FLUENT for instance.

#### 3.1.2 Modeling in COMSOL 5.2a and global approach

**Modeling process** The modeling process in COMSOL 5.2a consists in several steps :

- Building a geometry (Fig. 3.1)
- Defining a material to each domain of the geometry

- Choosing one of the available modules<sup>1</sup> depending on the physical problem to model
- Setting the boundary conditions on each boundary of the system
- Creating a mesh
- Running calculations
- Studying the results

**Global approach** The global approach of this thesis work consists in the following steps.

1. Creating a model for a chosen solar dryer
2. Validating the model by comparing with on-site measurements
3. Using the model to give ideas for design optimization

## 3.2 Assumptions

1. The solar dryers' studies are steady state <sup>2</sup> for a constant solar irradiation. This is an approximation since the solar irradiation varies with time and weather conditions (clouds).
2. The calculations can be run on half of the solar dryer without affecting the accuracy of the results given the symmetry <sup>3</sup> of the considered geometry.
3. The solar dryers which are modeled are built with a black net put on top of the absorber. This net is neglected.
4. The plastic sheet does not absorb visible radiation ( $a_p = 0$ ). It only reflects and transmits it.
5. The outward radiation from the sides is assumed to be radiated toward the sky while the radiation from the bottom goes to the ground.

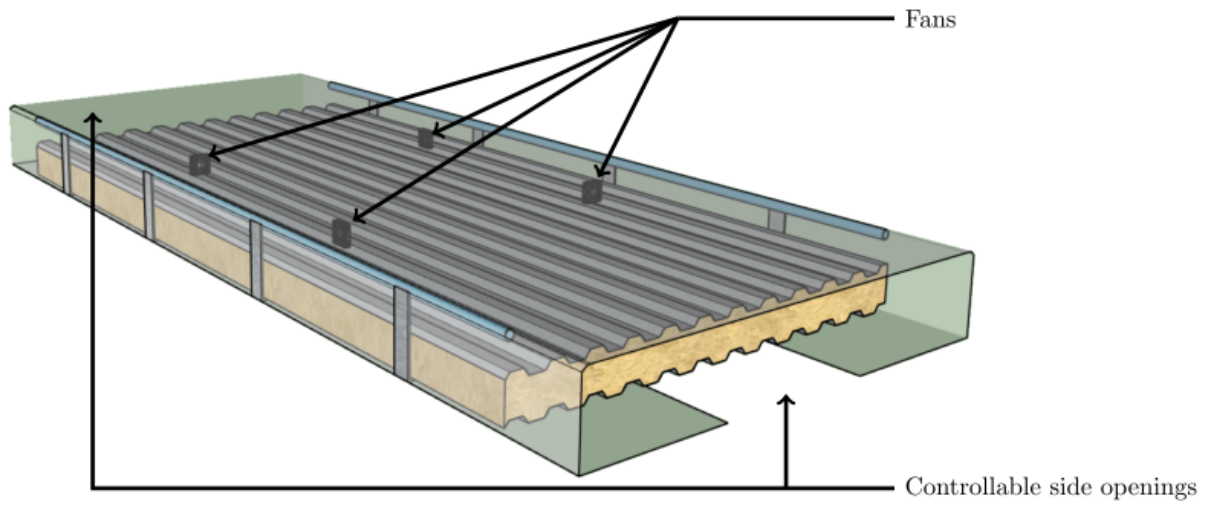
---

<sup>1</sup>A module in COMSOL corresponds to a set of equations and boundary conditions for a specific field in physics. Some examples of modules are : Heat Transfer in Solids, Laminar Flow, Turbulent Flow

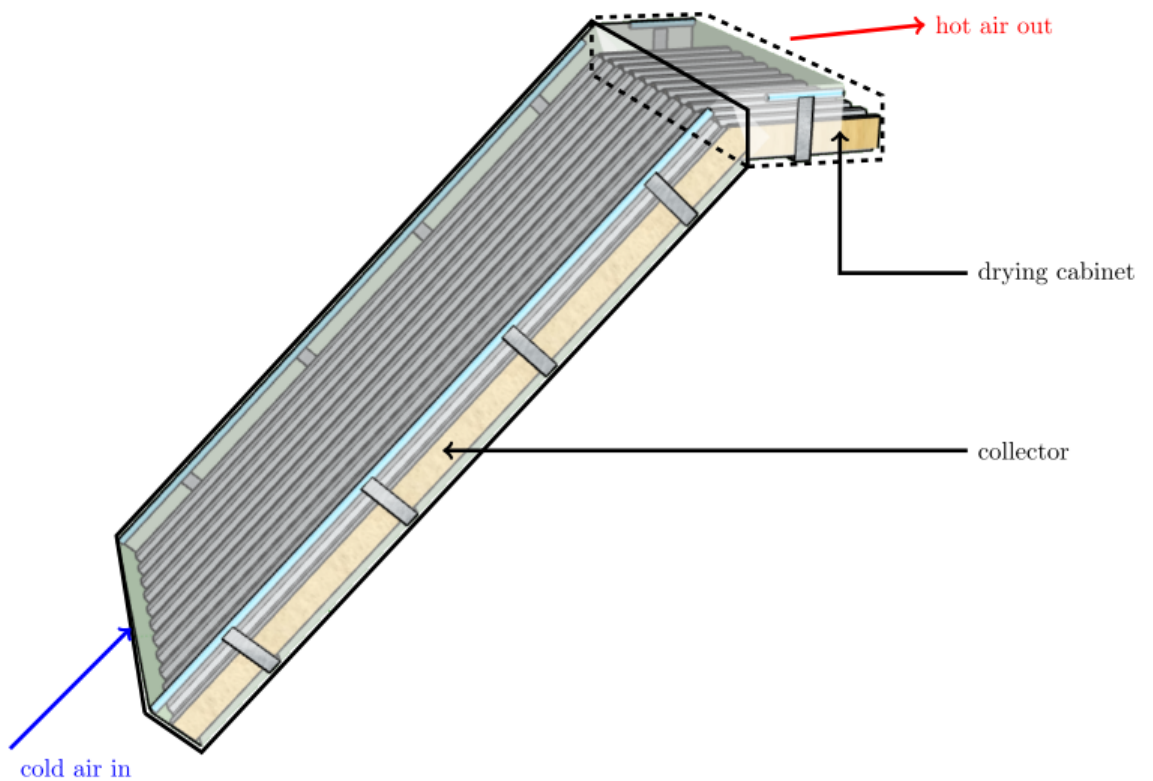
<sup>2</sup>The solar dryers are estimated to reach their final temperatures in about half an hour, based on the on-site tests in Mozambique

<sup>3</sup>The solar dryer is symmetric along the axis going from the center of the inlet side to the center of the outlet side

6. The heat radiation between the absorber and the plastic sheet is taken into account and a view factor is calculated for this
7. The inner sides are assumed not to reflect radiation, given their relative size and temperature.
8. There are no air leakages.



(a) Geometry of the active solar dryer to be modeled



(b) Geometry of the passive solar dryer to be modeled

Figure 3.1: Schematics of the solar dryers modeled in COMSOL - Images courtesy of Etienne Deslandes and Peter Samuelsson



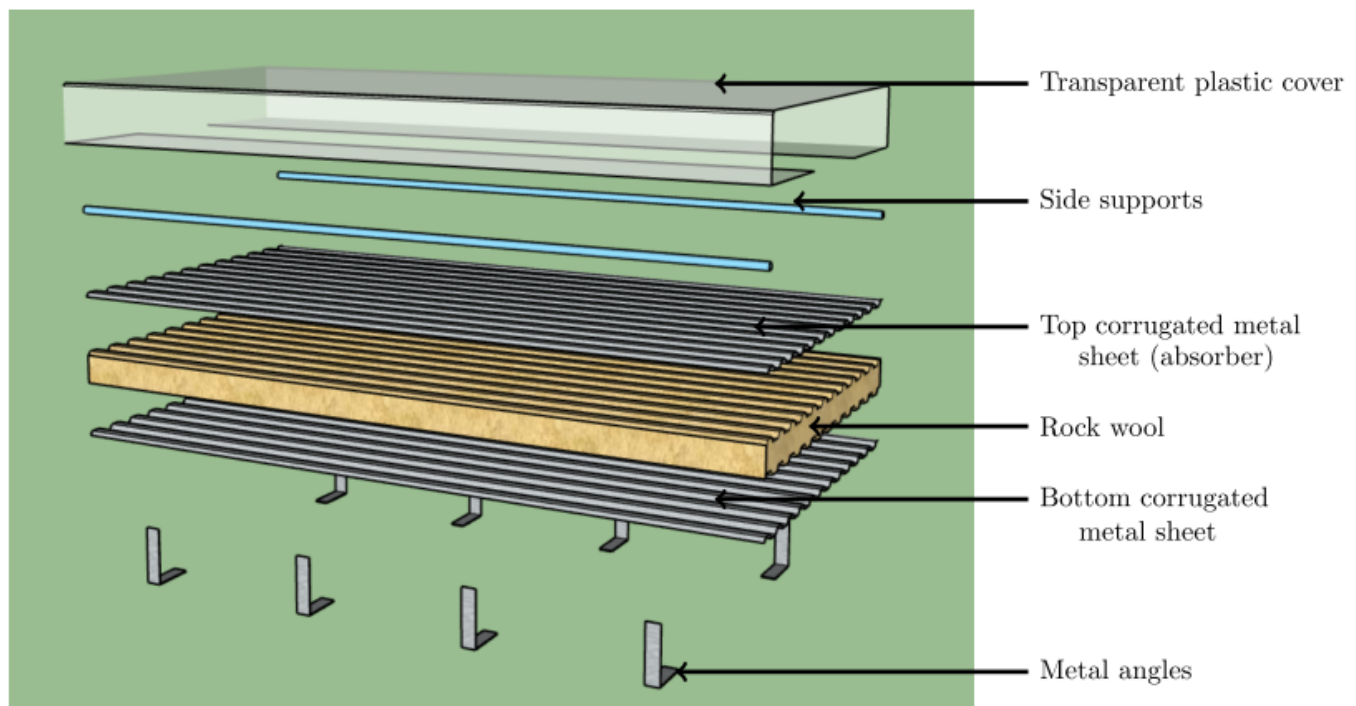


Figure 3.2: Exploded view of the solar dryers - Image courtesy of Etienne Deslandes and Peter Samuelsson

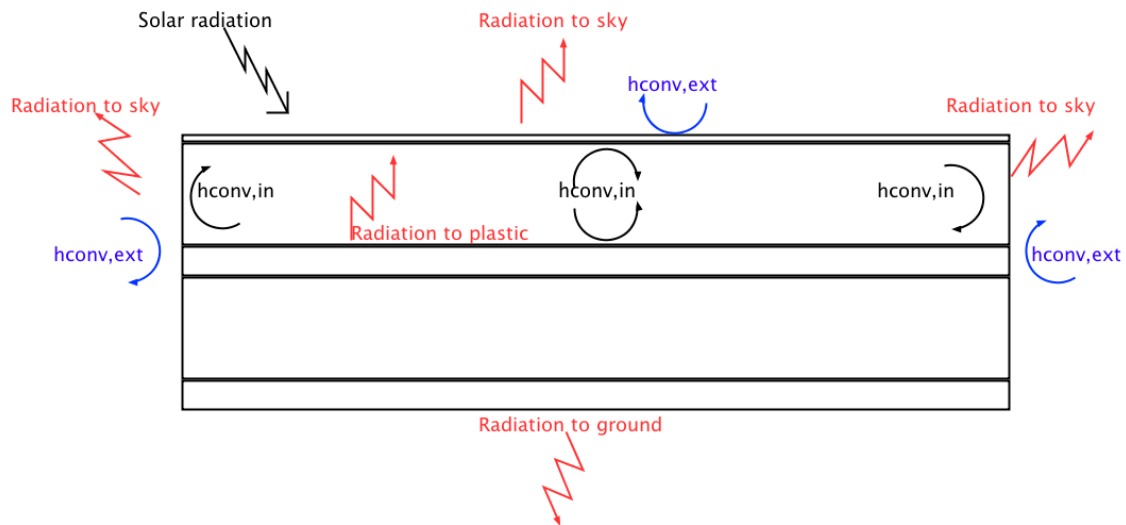


Figure 3.3: Schematics of the heat transfer exchange in a solar dryer cross-section

## 3.3 Theory

### 3.3.1 Heat transfer

**Heat transfer in a solar dryer** The heat transfer exchanges in a solar dryer are presented on Figure 3.3. The solar radiation is transmitted through a plastic sheet and absorbed by the absorber plate. Once the radiation is absorbed, part of it is emitted back to the plastic sheet. The rest is used to heat the air by convection on the absorber plate and the inner sides. The role of the absorber is thus to convert radiation in heat, by absorption and emission. Convection also happens on the plastic sheet and the outer sides with the ambient air. Losses occur by radiation from the plastic sheet from the sides of the solar dryer to the sky and from the bottom sheet of the collector to the ground. Finally, heat is transferred by conduction in the different materials.

**Heat transfer equation** The Heat Transfer module is used in COMSOL to determine the physics of the dryer (air velocity, air temperature, plastic sheet temperature, absorber temperature, bottom part temperature, pressure, etc). This module can be coupled with the non-isothermal flow module in order to study heat transfer on a domain including fluid and solid parts.

The heat transfer phenomena in the solar dryer are due to three main effects : conduction, convection and radiation. The Heat Transfer Module in COMSOL aims to solve the heat equation (Eq.3.1) finding the value of the temperature  $T$  (Multiphysics 2012, p. 31).

As the problem is assumed to be stationary, the following equation (Eq. 3.1) can be written as follow :

$$\rho C_p u \nabla T + \nabla \cdot q = Q \quad (3.1)$$

Where :

- $\nabla$  is the gradient operator <sup>4</sup>
- $\rho$  is the density (SI unit : kg/m<sup>3</sup>)
- $C_p$  is the specific heat at constant pressure (SI unit : J/kg · K)
- $T$  is the absolute temperature (SI unit : K)
- $u$  is the velocity vector (SI unit : m/s)
- $q$  is the heat flux by conduction (SI unit : W/m<sup>2</sup>) calculated with the Fourier law

$$q = -k \nabla T \quad (3.3)$$

- $k$  is the thermal conductivity (SI unit : W/m·K)
- $Q$  represents the heat sources (SI unit : W/m<sup>3</sup>)

### 3.3.2 Solar radiation

The solar dryer working principle relies on the use of solar radiation. When sun radiation  $G$  (W/m<sup>2</sup>) hits on the plastic sheet part of it is absorbed by the plastic sheet. However, in the modeling, this absorption is neglected. Then, another part of the solar radiation is reflected (depending on the reflection coefficient  $R_p$ ) and the remaining part is transmitted through the plastic sheet depending on the transmission coefficient  $\tau_p$ . The radiation is then absorbed by the absorber depending on the absorption coefficient  $\alpha_{abs}$  and reflected depending on  $R_{abs}$ .

---

<sup>4</sup>Considering  $A$  a mathematical function, its gradient in a three dimensions space with the three director vectors  $\mathbf{x}$ ,  $\mathbf{y}$ ,  $\mathbf{z}$ . Then, it is possible to define the gradient of  $A$  as :

$$\nabla A = \frac{\partial A}{\partial x} \mathbf{x} + \frac{\partial A}{\partial y} \mathbf{y} + \frac{\partial A}{\partial z} \mathbf{z} \quad (3.2)$$

It is thus possible to model the solar radiation by a heat source applied on the absorber which value is  $G_e$ , calculated using the following equation (equation 3.4). This equation takes into account the multiple reflections between the plastic sheet and the absorber.

$$G_e = \frac{G\tau_p\alpha_{abs}}{1 - R_pR_{abs}} \quad (3.4)$$

### 3.3.3 Convective heat transfer coefficient

**External convection** A previous modeling work (Olsson 2016) made the assumption that the convective heat transfer coefficient  $h_{conv,out}$  would be constant and equal to  $20 \text{ W/m}^2 \cdot \text{K}$ . However, it is possible to use predefined options for external natural convection in COMSOL based on the values of the length or height of the considered area and on the ambient temperature.

Convection effects occurring on the plastic sheet refer to a case of external natural convection on a horizontal plate (upside). Since the plastic sheet receives radiation from the absorber (cf. Section 3.4.5 below), it is assumed that it has a temperature  $T_{plast}$  greater than the ambient temperature  $T_{amb}$ . Thus, the convective heat transfer coefficient will be calculated according to (3.5).

$$h = \begin{cases} \frac{k}{L} 0.54 Ra_L^{\frac{1}{4}} & Ra_L \leq 10^7 \\ \frac{k}{L} 0.15 Ra_L^{\frac{1}{3}} & Ra_L > 10^7 \end{cases} \quad (3.5)$$

The Rayleigh number  $Ra_L$  is given by 3.6 and  $L$  refers to the plate diameter equal to the ratio between its area and perimeter. The material data is evaluated for a temperature of  $\frac{T+T_{ext}}{2}$ , where  $T_{ext}$  is the temperature outside of the solar dryer. In this case, for external convection, it would be the temperature of the surroundings  $T_{amb}$ .

$$Ra_L = \frac{g | (\frac{\partial \rho}{\partial T})_p | \rho C_p | T - T_{ext} | L^3}{k\mu} \quad (3.6)$$

where  $g$  is the gravity acceleration equal to  $9.81 \text{ m/s}^2$ .

For the external convective heat transfer on the collector sides, the sides walls are considered as vertical walls. The Rayleigh number  $Ra_L$  is calculated taking  $L$  equal to the height of the wall using Equation 3.6 again. Then the convective heat transfer coefficient

is given by (3.7).

$$h = \begin{cases} \frac{k}{L} \left( 0.68 + \frac{0.67 Ra_L^{\frac{1}{4}}}{\left(1 + \left(\frac{0.492k}{\mu C_p}\right)^{\frac{9}{16}}\right)^{\frac{4}{9}}} \right) & Ra_L \leq 10^9 \\ \frac{k}{L} \left( 0.825 + \frac{0.387 Ra_L^{\frac{1}{6}}}{\left(1 + \left(\frac{0.492k}{\mu C_p}\right)^{\frac{9}{16}}\right)^{\frac{8}{27}}} \right)^2 & Ra_L > 10^9 \end{cases} \quad (3.7)$$

The use of these heat transfer coefficients instead of a constant value aims to enhance the accuracy of the modeling.

**Internal convection** Convection occurs inside the collector due to interaction between the air circulation and the downside of the plastic sheet, the upside of the absorber and the inner sides of the collector made of plastic too. As a first approximation, it is possible to assume that the airflow in the solar dryer is a turbulent airflow in a smooth circular tube. However, an effective diameter named hydraulic diameter  $D_h$  instead of using the circular tube diameter  $D$  as the characteristic length. It is defined in equation 3.8.

$$D_h = \frac{4A_c}{P} = \frac{2(lh)}{l+h} \quad (3.8)$$

where  $A_c = wh$  and  $P = 2(w+h)$  are respectively the flow cross-sectional area and the perimeter with  $w$  and  $h$  the width and height of the flow cross-sectional area.

It is possible to use the following empirical correlations to evaluate the Nusselt number of the flow and thus the intern convective heat transfer coefficient (Incropera, F.P. and Dewitt, D.P. 2002, p.491-492). For Reynolds numbers between 3000 and  $5 \cdot 10^6$  and for  $0.5 < Pr < 2000$ , it is possible to use a correlation proposed by Gnielinski (see equation 3.9).

$$Nu_D = \frac{\left(\frac{f}{8}\right)(Re_D - 1000)Pr}{1 + 12.7\left(\frac{f}{8}\right)^{1/2}(Pr^{2/3} - 1)} \quad (3.9)$$

$f$  is the Moody (or Darcy) friction factor. This factor is defined by equation 3.10 but can also be calculated thanks to the correlation of equation 3.11, valid for  $3000 < Re_D < 5 \cdot 10^6$  (Incropera, F.P. and Dewitt, D.P. 2002, p.470).

$$f = \frac{-(dp/dx)D}{\rho u_m^2/2} \quad (3.10)$$

$$f = (0.790 \ln(Re_D) - 1.64)^{-2} \quad (3.11)$$

Finally, once the friction factor and then the Nusselt number are calculated for properties of the airflow evaluated for the average temperature  $T_m$ , it is possible to estimate the convective heat transfer coefficient (Eq.3.12).

$$Nu = \frac{h_{conv,in}\lambda_{air}}{D_h} \quad (3.12)$$

### 3.3.4 Radiative heat transfer

Radiative heat transfer is an essential phenomenon regarding the working principle of a solar dryer. It includes both radiative heat transfer with the ambient surroundings and between surfaces. The radiation between the plastic sheet and the absorber plate have to be taken into account for the design of the aforementioned solar dryer.

#### Radiation to ambient

A first level of analysis for radiative heat transfer is to take into account the radiation from a surface to the ambient surroundings. On a considered surface  $x$ ,  $G$  is the inward heat flux received by this surface and the radiosity  $J$  is the outgoing radiative heat flux defined in equation 3.13. The surface  $x$  is characterized by its reflectivity  $\rho$ , its absorptivity  $\alpha$  and its emissivity  $\epsilon$ .  $\sigma$  is the Stefan-Boltzmann constant equal to  $5,67 \cdot 10^{-8} \text{ W/m}^2 \cdot \text{K}^4$ .

$$J = \rho G + \epsilon \sigma T^4 \quad (3.13)$$

The net inward radiative heat flux  $q$  is thus the difference between the incoming heat flux  $G$  and the radiosity  $J$  as expressed by equation 3.14.

$$q = G - J = (1 - \rho)G - \epsilon \sigma T^4 \quad (3.14)$$

In the radiation to ambient case, the ambient surroundings of the surface are considered to be seen equally from this surface and with a constant temperature  $T_{amb}$ . The ambient surroundings are assumed to behave as a blackbody and according to equation 3.15, it is possible to obtain a simple expression of  $G$  and of the net inward heat flux  $q$  as well (eq. 3.16).

$$G = \sigma T_{amb}^4 \quad (3.15)$$

$$q = \epsilon \sigma (T_{amb}^4 - T^4) \quad (3.16)$$

### Surface-to-surface radiation

The surface-to-surface boundary condition in COMSOL Multiphysics enables to take into account both the radiation from the ambient surroundings and from other surfaces (Multiphysics 2012). For such a case, the equation of the irradiative flux on the concerned surface is given by Eq.3.17.

$$G = G_m + \sigma F_{amb} T_{amb}^4 \quad (3.17)$$

**Mutual irradiation** In equation 3.17,  $G_m$  accounts for the mutual irradiation received from the other surfaces. It is calculated according to the following equation (3.18) :

$$G_m = \int_{S_2} \frac{(\bar{n}_1 \cdot \bar{r})(-\bar{n}_2 \cdot \bar{r})}{\pi |\bar{r}|^2} J_2 dS_2 \quad (3.18)$$

Considering two surfaces named S1 and S2, a point  $x_1$  on S1 sees the radiation from the points on S2. Each point on S2 is assumed to have a radiosity value  $J_2$  while the surroundings remain at a constant temperature  $T_{amb}$ . Then, the vector  $\bar{r}$  points from a point  $x_1$  on S1 to a point  $x_2$  on S2. The heat flux received from  $x_2$  depends on the local radiosity at this points  $J_2$  projected onto  $x_1$ . The projection is operated between the normal vectors  $\bar{n}_1$  and  $\bar{n}_2$  along with the vector  $\bar{r}$ . The equation can be extended to the case where there are many surfaces. Then, all the indexes 2 would be removed and  $S$  would represent all the other surfaces of the geometry (Multiphysics 2012).

**View factor** Radiative heat transfer between surfaces depends on the orientation of these surfaces and the view factor aims to represents this dependence. It depicts the portion of radiation leaving one surface that strikes another surface (Cengel, Y., Cimbala, J. and Turner, R. 2012). For instance, when calculating the irradiative flux leaving S1, the view factor  $F_{12}$  would be equal to the fraction of the radiation leaving S1 that strikes S2.

The ambient view factor quantifies the portion of radiative heat exchange of a surface with the ambient surroundings and is given by the equation 3.19 below.

$$F_{amb} = 1 - \int_S \frac{(\bar{n}_1 \cdot \bar{r})(-\bar{n}_2 \cdot \bar{r})}{\pi |\bar{r}|^2} dS \quad (3.19)$$

### 3.3.5 Drying process

The last phenomenon to model is the drying of the SAP pouches in the solar dryers. Based on the data provided by (Olsson 2016), it is possible to calculate the mass flow of water evaporated from a pouch and the energy needed to evaporate water from a SAP pouch (equations 3.20 and 3.21). However, these calculations are done for bags containing water (and not fruit juice).

$$m_{vap} = \frac{A_{bags}}{3600} \cdot (-1,0015 \cdot u_{bags} - 0,9565) \cdot RH + 0,3088 \cdot u_{bags} + 0,6297 \quad (3.20)$$

$$E_{vap} = m_{vap} \Delta H_{vap} \quad (3.21)$$

## 3.4 Models description

### 3.4.1 Geometry

The dryer is built as a "sandwich" structure made of :

- plastic
- metal sheet absorber
- rock wool
- metal sheet (bottom)

The different parts are hold together thanks to metal pieces that are not taken into account in the model. We assume that the sides of the collector are only made of plastic. The dryer performances will be tested in laboratory for two different configurations :

- Passive tilted dryer ( $\theta = 45^\circ$ )
- Active flat dryer, using fans



### 3.4.2 Models description

#### Model 1 : Tilted collector without airflow study

Model 1 aims to represent the tilted collector shown on Figure 3.1b, with a tilt angle of  $\theta = 45^\circ$ . It is a passive collector in which natural convection occurs. A first model of this solar dryer consists in quantifying heat transfer. In this model, the air inlet velocity is set to a constant value in the whole collector. It results in the use of the Heat Transfer Module in COMSOL. In this model, the study focuses on the air characteristics at the outlet of the collector (temperature distribution, relative humidity). The airflow is not modeled using fluid dynamics equation, the airflow velocity value is used to calculate the Nusselt number and deduce the convective heat transfer occurring on the absorber plate.

#### Model 2 : Flat active collector with SAP pouches inside

It is interesting to model an active dryer, shown on Figure 3.1a, containing bags full of water. To do so, the Heat Transfer Module is again used in COMSOL. In this model, the solar dryer is the same as the indirect solar dryer, except that the direct solar dryer is flat and the bags are put directly in the solar dryer. The temperature distribution in the dryer and the relative humidity are the two main parameters studied.

### 3.4.3 Materials

The physical properties of the materials have been chosen approximately and relying on the materials bank in COMSOL. The material properties are given in Table 3.1.

Material	Density (kg/m <sup>3</sup> )	Dynamic Viscosity (Pa · s)	Constant specific heat (J/kg/K)	Thermal conductivity (W/m/K)	Surface emissivity
Air	$\rho(T, p)$	$\eta(T)$	$C_p(T)$	$k(T)$	/
Structural steel	7859	/	475	44.5	0.92
Rock wool	114	/	840	0.033	/
Acrylic plastic	1190	/	1470	0.18	0.8

Table 3.1: Materials' properties

Air properties are temperature-dependent and calculated by COMSOL. The values for rockwool properties were found in SIPER 2011 and the surface emissivity value for structural steel was given by TataSteel 2014.

### 3.4.4 Ambient data

COMSOL offers the possibility to set ambient temperature, pressure, relative humidity and wind speed based on meteorological data. In the following models, the meteorological data are taken in the station of Maputo, Mozambique at the date of June, 1st (12:00). The average temperature is defined as ambient temperature and so on for the other parameters. To calibrate the model, the ambient conditions were measured on-site in Inharrime and used for the simulation.

### 3.4.5 Heat transfer module boundary conditions (Model 1)

**Absorber** All the phenomena taken into account for the absorber equation are presented in Table 3.2. The absorber receives the solar radiation coming from the sun through the plastic as stated before. It is easier and accurate enough to model the effective power  $G_e$  received by the absorber. It acts as a heat source boundary condition in this model. The absorber also sends radiation to the plastic sheet.

Heat transfer occurs as well by convection between the absorber surface and the air circulating between the absorber and the plastic sheet. The convective heat transfer coefficient  $h_{conv,in}$  is calculated as explained in Section 3.3.3.

The heat transfer due to conduction through the sides and the rock wool under the absorber is calculated thanks to the materials conductivity and the temperature gradient between these areas (Eq.3.1).

Phenomenon	Heat transfer	COMSOL modeling
Heat source	$G_e$	Boundary condition : Boundary Heat Source Surface selected : Absorber top Settings : $G_e$ (W/m <sup>2</sup> )
Convection with air inside	$-h_{conv,in}(T_{abs} - T_{air})$	Boundary condition : Boundary heat source Surface selected : Absorber Settings : $h_{conv,in} = \frac{k_{air}Nu}{D_h}$ $Q_0 = h_{in}(T - T_{air})$
Radiation sent to plastic	see Eq.3.17	Boundary condition : Diffuse surface Surface selected : Absorber Settings : $\epsilon_{abs}$ and $T_{ambient,COMSOL} = T_{air}$
Conduction	see General Equations	Settings : $k$ defined in Materials

Table 3.2: Absorber heat transfer

**Plastic sheet** All the boundary conditions on the plastic sheet are given in Table 3.3. The ambient air at a temperature of  $T_{amb}$  is responsible for external convection on the plastic sheet. Convection occurs on the other side of the plastic sheet, due to the air circulation at a mean temperature equal to  $T_{air}$  inside the solar dryer. The heat transfer convection coefficient  $h_{conv,out}$  and  $h_{conv,in}$  are calculated as explained in Section 3.3.3. The plastic sheet then receives radiation from the absorber.

Phenomenon	Heat transfer	COMSOL modeling
External convection	$-h_{con,out}(T_p - T_{amb})$	Boundary condition : Heat flux - Convection Surface selected : Plastic out Settings : $h_{con,out}$
Convection on the inner side	$+h_{con,in}(T_{air} - T_p)$	Boundary condition : Boundary heat source Surface selected : Plastic in Settings : $h_{conv,in} = \frac{k_{air}Nu}{D_h}$ $Q_0 = h_{in}(T_{air} - T)$
Radiation received from absorber	$+\epsilon_p(G - \sigma T^4)$	Boundary condition : Surface-to-surface diffuse Surface selected : Plastic in Settings : $\epsilon_p$ , Ambient temperature $T_{amb}$
Radiation to the sky	$-\epsilon_p\sigma(T_p^4 - T_{sky}^4)$	Boundary condition : Diffuse surface Surface selected : Plastic out + walls out Settings : $\epsilon_p$

Table 3.3: Plastic sheet heat transfer

**Sides and bottom** Convection occurs on the external sides made of plastic sheet again. The convection heat transfer coefficient is obtained through the correlations for external convection on a vertical wall. There is convection on the inner side of the plastic sheet as well with the coefficient  $h_{in}$  calculated exactly as done before for the internal convection.

Radiative heat transfer also needs to be taken into account. The heat is radiated to the sky but also to the ground. The assumption made in this model is that the sides send radiation to the sky while the bottom part of the solar dryer made from metal sheet irradiates toward the ground.

The heat transfer by conduction is calculated knowing the conductivity of materials and the temperature gradients. All these phenomena are gathered in Table 3.4.

Phenomenon	Heat Transfer	COMSOL Modelling
Convection outside plastic sides	$-h_{conv,out}(T_p - T_{amb})$	Boundary condition : Heat flux - Convection Surface selected : Plastic out Settings : $h_{conv,out}$
Convection inside along plastic sides	$-h_{conv,in}(T_p - T_{air})$	Boundary condition : Boundary Heat Source Surface selected : Plastic in Settings : $h_{conv,in} = \frac{k_{air}Nu}{D_h}$ $Q_0 = h_{in}(T - T_{air})$
Radiation sky	$-\epsilon_p\sigma(T_p^4 - T_{sky}^4)$ to the	Boundary condition : Diffuse surface-to-surface Surface selected: Plastic out Settings : $\epsilon_p$ and $T_{ambient,COMSOL} = T_{air}$
Radiation to the ground	$-\epsilon_{abs}(T_{bottom}^4 - T_{sky}^4)$	Boundary condition : Diffuse surface-to-ambient Surface selected : bottom Settings: $\epsilon_{abs}$ and $T_{ambient,COMSOL} = T_{sky}$
Conduction	see General Equations	Settings : $k$ defined in materials

Table 3.4: Sides and bottom heat transfer

### 3.4.6 Heat transfer module boundary conditions (Model 2)

To model the flat active dryer with SAP pouches inside, the previous boundary conditions used for Model 1 are kept. Boundary conditions are added to take into account the energy absorbed by the bags, defined by a boundary heat source. The direct radiation received by the bags is not modeled. The convection on the bags due to airflow is thus taken into account.

## 3.5 Model validation

To validate the accuracy of the modeling work, it is possible to compare the results obtained through the model to measurements on the solar dryer which is aimed to be optimized. The measures were taken on-site in Inharrime, Mozambique, on the 13th of June, 2017 between 11h and 14h.

### 3.5.1 Measurement tools

The measurements collected are temperatures and relative humidity at chosen points on the solar dryer. To do so, two measurements tools have been used :

- Four Vernier© sensors patched on strategic points on the solar dryer
- an Testo probe connected to a Testo435-2 logger, able to measure temperature and relative humidity as well

The measurements were taken during 30 minutes to reach stable values. The logs were stored on the Vernier © device and then transferred to a computer to be exploited on Excel. Each measurement has been done twice to deal with the repeatability aspects of the experiments.

### 3.5.2 Experimental set-up

As shown on Figure 3.4, the sensors are placed at chosen points and held thank to adhesive tape. The measurements points are presented on Figure 3.5, for the tilted collector. However, the same points are taken as reference on the outlet surface of the flat collector. The measurement points are numbered and will be referred by their number later. All the measurements are done on the outlet surface of the collector.

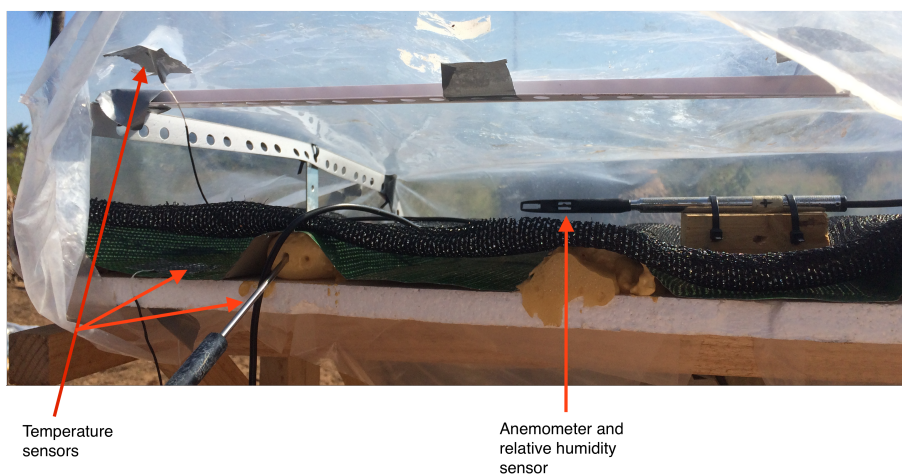


Figure 3.4: Pictures of experimental set-up and measurement tools

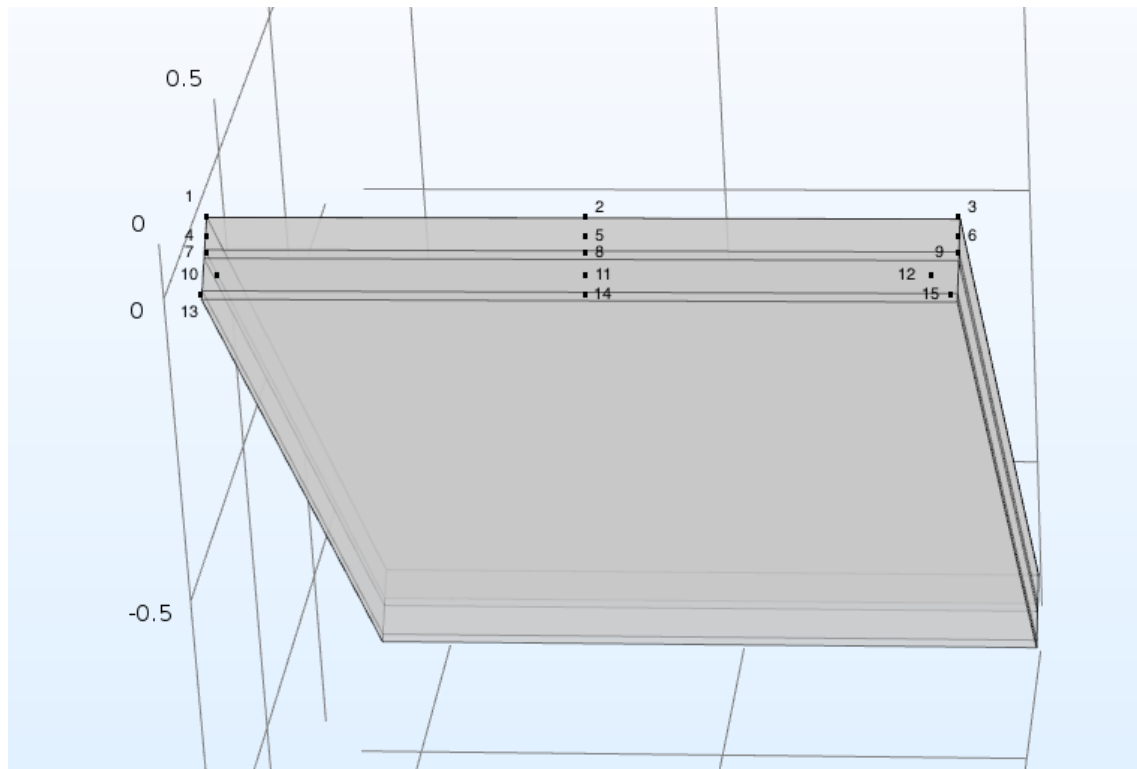


Figure 3.5: Schematics of the outlet of the solar dryer and identified points of measurements

The relative humidity is measured only for points 4,5,6 which corresponds to measurements of the outlet air characteristics.

The ambient conditions were measured during 3 hours. Then, an average of the ambient temperature, ambient relative humidity and ambient solar irradiation has been done and used as initial values in the COMSOL© models.

### 3.5.3 Relative error

Comparing actual measurements and modelling results aims to evaluate the global accuracy of the models. For this reason, a relative error calculation is taken on to quantify the accuracy of the model. More complex mathematical tools could be available but they are not relevant for this present thesis. The relative error is defined by Equation 3.22.

$$RelErr = \frac{x_{experimental} - x_{theoretical}}{|x_{theoretical}|} \quad (3.22)$$

# Chapter 4

## Results

*The chapter aims to present the results of the modeling work. The models are compared with measurements carried out on actual solar dryers. Some optimization is proposed for its design thanks to parametric studies done with the modeling tools.*

### 4.1 Tilted passive solar dryer

#### 4.1.1 Initial values

The data regarding ambient conditions (ambient temperature, relative humidity, solar irradiance) were measured on-site in Inharrime (Mozambique) and used as input values for the model. The ambient temperature, relative humidity and solar irradiance are thus known as well as the material properties of the solar dryer components. These materials are locally produced and the access to accurate technical data sheet is not easy. However, as it will be shown later, not all the material properties have a high influence on the simulation results. The table 4.1 below gathers all the specific values used as input data for the modeling of a tilted passive solar dryer in Inharrime (working hours : from 11h to 13h). The materials properties are given in Table 3.1.

#### 4.1.2 Temperature profiles

It is possible to obtain the temperature profiles along the length of the collector, at different heights. The lines taken to plot these temperature profiles are shown on Figure 4.1 colored in red. Half of the collector is represented on this figure. The lines are contained in the symmetry plan of the collector ( $x = l/2$ ). The temperature profiles along these lines can

Parameter	Value	Unit
$w_{col}$	1,1	m
$l_{col}$	1,8	m
$t_{gap}$	0,05	m
$t_{insulation}$	0,05	m
$t_{metal}$	1,80	cm
$t_{plast}$	0,10	mm
$G$	916,1	W/m <sup>2</sup>
$\tau_{plastic}$	0,7	-
$\alpha_{absorber}$	0,6	-
$R_{plastic}$	0,1	-
$R_{absorber}$	0,27	-
$T_{amb}$	31,6	°C
$RH_{amb}$	34,4	%

Table 4.1: Input data for tilted passive solar dryer in Inharrime

be seen on Figure 4.3.

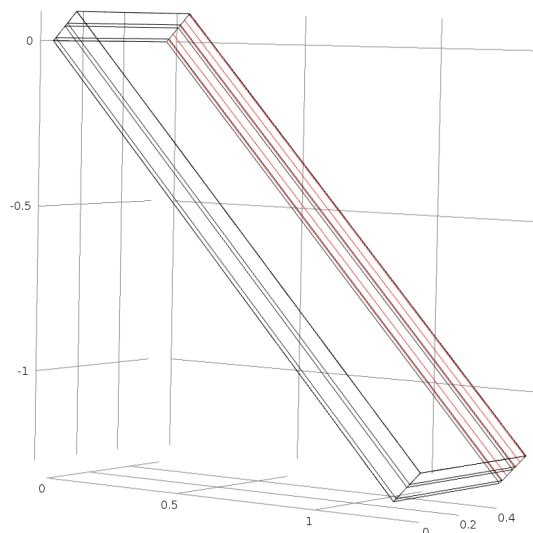


Figure 4.1: Reference lines used to plot the temperature profiles



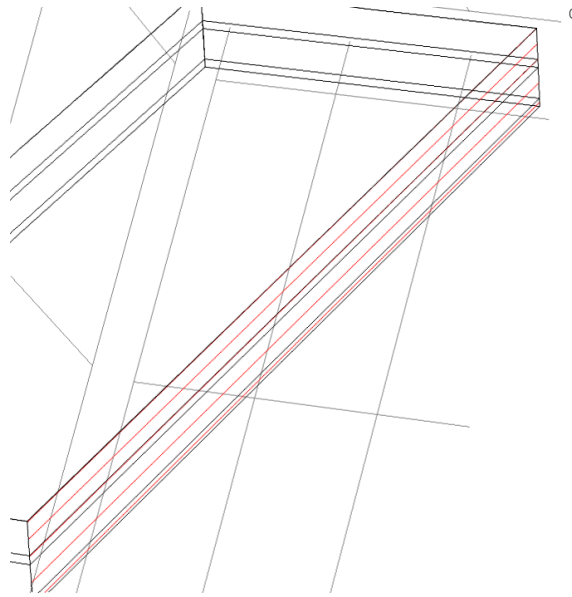


Figure 4.2: Zoom on the reference lines used to plot the temperature profiles

The temperatures reached by the collector at its outlet are presented in Table 4.2.

Element	Plastic sheet	Air ( $t_{\text{gap}}/2$ )	Absorber	Insulation (2,5 cm)	Bottom
Temperature (°C) outlet surface	55,2	59,5	76,0	43,0	33,2

Table 4.2: Temperatures of the different elements at the outlet of the collector

The air temperature is above 50 °C and below 65 °C which means that the drying is performed in the correct range of temperatures mentioned in Section 2.3.3 to ensure the quality of the drying product.

The temperature profiles on Figure 4.3 shows that these different temperatures increases from the ambient temperature, except for the plastic sheet. Less than 15 % of the collector length is necessary for the different elements to reach 80 % of the outlet temperature.

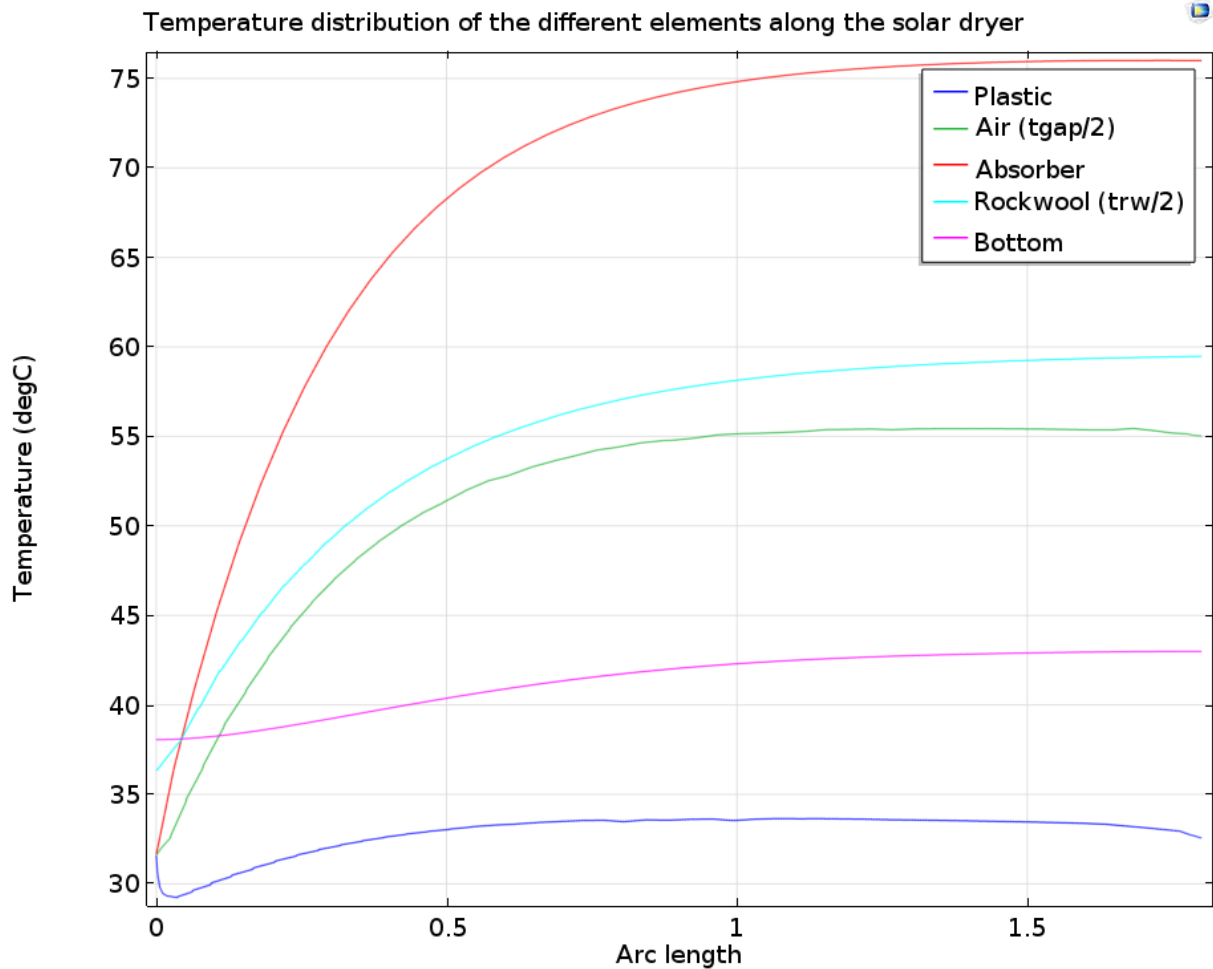


Figure 4.3: Temperature profiles - Tilted passive solar dryer

### 4.1.3 Convection coefficient

Five convective heat transfer coefficient can be evaluated in Table 4.3.

Convective Heat transfer Coefficient type	External topside plastic	External plastic sides	Internal Absorber	Internal Plastic inner side	Internal Inner sides
Value ( $W/m^2 \cdot K$ )	1,21	19,8	4,5	1,28	0,11

Table 4.3: Convective heat transfer coefficient

The convection coefficient for the heat transfer with the air inside the solar dryer is twenty times lower than the convection coefficient for the external convection. The con-

vection on the inside walls of the solar dryer are negligible.

The influence of the value of these coefficients is studied in Section 4.2.2 and the value for the internal convection heat transfer coefficients will be discussed as well.

#### 4.1.4 Relative humidity

The average ambient relative humidity given by the meteorological data is 54 %. However, the value measured on-site is 34,4 % and is the one which is used in simulations. The calculations done by COMSOL show that at the outlet of the collector, the relative humidity drops to 10,1 % at the center of the air outlet surface. The relative humidity increases as the air is close to the plastic sheet and is lower on the absorber, probably because it is where the temperature is higher.

The drop in relative humidity is essential to ensure the drying of the SAP-pouches in the solar dryer. If the humidity rate would be too high inside the solar dryer, the water contained in the juice could not evaporate and the drying could not occur. The SAP-pouches are put on the absorber, in a small horizontal drying chamber joined to the passive tilted collector. The air passing around the pouches has the smallest humidity rate which favours the drying process.

#### 4.1.5 Energy balance

The energy balance terms are detailed in Table 4.4 below. Losses are counted as negative and gains are positive.

Surface	Phenomena	Equation	Value (W)
Plastic sheet	External convection	$A_{abs}h_{conv,out}(T_p - T_{amb})$	- 18,59
	Radiation	$h_{rad,out}A_{abs}(T_p - T_{sky})$	- 123,38
	Total plastic sheet		- 141,97
Sides	External convection	$h_{conv,out}A_{sides}(T_{side} - T_{amb})$	-54,6
	Radiation	$h_{rad,out}A_{sides}(T_{sides} - T_{sky})$	-42,4
	Total sides		-97
Bottom	Radiation	$h_{rad,out}A_{abs}(T_{bottom} - T_{amb})$	-13,0
Air	Heated by absorber	$X(T_{out} - T_{in}) + m_h C_{p,vap}(T_{out} - T_{in})$	-91,4
Absorber	Heat source	$G_e$	329,6
Efficiency of the dryer	-	$\frac{X(T_{out}-T_{in})+m_h C_{p,vap}(T_{out}-T_{in})}{G_e * A_{abs}}$	0,28

Table 4.4: Energy balance of the tilted passive solar dryer on half on the collector

This balance is done on half of the solar dryer but would of course be the same for the entire solar dryer thanks to a symmetry condition. The efficiency of 28 % seems to be a reasonable value when compared to the results found in (Hegde, V.N., Hosur, V.S., Rathod, S.K., Harsoor, P.A. and Narayana, K.B. 2015) for the same kind of solar dryer.

#### 4.1.6 Comparison with on-site measurements

The relative humidity measured for the outlet air was in average 12 % and the model gives an average of 11 %. The relative humidity is thus well estimated by the model in average.

This model gives a relative error below 15 % for the air temperature (with a temperature of reference in °C), insulation temperature and the bottom temperature. However, the temperature on the sides of the collector are more difficult to estimate in general, except for the absorber.

Point #	Component	Measurement	Model 1	Relative error (Celsius based)
1	Plastic sheet (L)	47,0 °C	35,4 °C	24,7 %
2	Plastic sheet (C)	46,6 °C	33 °C	29,2 %
3	Plastic sheet (R)	43,5 °C	35 °C	19,5 %
4	Air (L)	57,7 °C	50,7 °C	13,8 %
5	Air (C)	59 °C	55,2 °C	6,9 %
6	Air (R)	58,5 °C	51 °C	12,8 %
7	Absorber (L)	59,7 °C	64 °C	6,7 %
8	Absorber (C)	63,7 °C	76 °C	17,7 %
9	Absorber (R)	60,5 °C	62,1 °C	2,6 %
10	Insulation (L)	61 °C	52,2 °C	14,4 %
11	Insulation (C)	60,7 °C	59,4 °C	2,2 %
12	Insulation (R)	61,7 °C	52,1 °C	15,6 %
13	Bottom (L)	39,2 °C	40 °C	2,3 %
14	Bottom (C)	41,7 °C	43 °C	3,1 %
15	Bottom (R)	38,9 °C	40 °C	2,8 %

Table 4.5: Comparison between model 1 and actual measurements for temperature

## 4.2 Parametric studies

The parametric studies were performed for the tilted passive solar dryer. However, it can be assumed that the influence of each parameter is the same for the active flat solar dryer. The reference case built in Section 4.1 is used and only one parameter is changed at a time to study its influence on the global results.

### 4.2.1 Airflow velocity

The airflow velocity is constant in the solar dryer. The influence of airflow velocity on the outlet temperatures, the internal convective heat transfer coefficient and the energy losses is studied. Six values of airflow velocity are studied : 0,1 ; 0,5 ; 1,0 ; 1,5 ; 2,0 ; 2,5 m/s.

The higher the velocity, the lower the air temperature will be at the outlet. The same is observed for the absorber temperature at the outlet. This is due to the increased convection effects when increasing the airflow velocity. The air circulates faster in the absorber sheet and the heat will be transferred faster.

The temperature of the outlet air decreases as a 3rd order polynomial function of the inlet velocity variation. Approximately 5 °C are lost for a 1 m/s increase of the inlet velocity. However, the temperature is always above 55 °C, which is better for the drying process since the juice inside the pouches has to be at a temperature between 50°C and 65 °C and if the air does not reach this temperature, it is obviously impossible for the juice to reach it too.

The relative humidity does not vary much as well and remains at about 10 % varying from 5 % for the lowest velocity to 12 % for the highest. Since the relative humidity depends on the temperature value, it is normal that a higher speed induces a higher relative humidity rate, because a higher airflow velocity is responsible for a lower temperature in the air.

The internal convective heat transfer coefficient is affected by a change in the inlet airflow velocity. It is higher when the velocity is higher as shown on Figure 4.4. The range of values for this coefficient remains around [0,5 ; 2,0]. In the later parametric study for this coefficient, larger values will be studied.

### 4.2.2 External convective heat transfer coefficient

The external convective heat transfer coefficient has a low impact on the global performances of the solar dryer. The simulations were done for  $h_{ext} = 5, 10, 15, 20, 30 \text{ W/m}^2 \cdot \text{K}$ . The temperature of the different elements of the solar dryer drops by 8 °C in average when

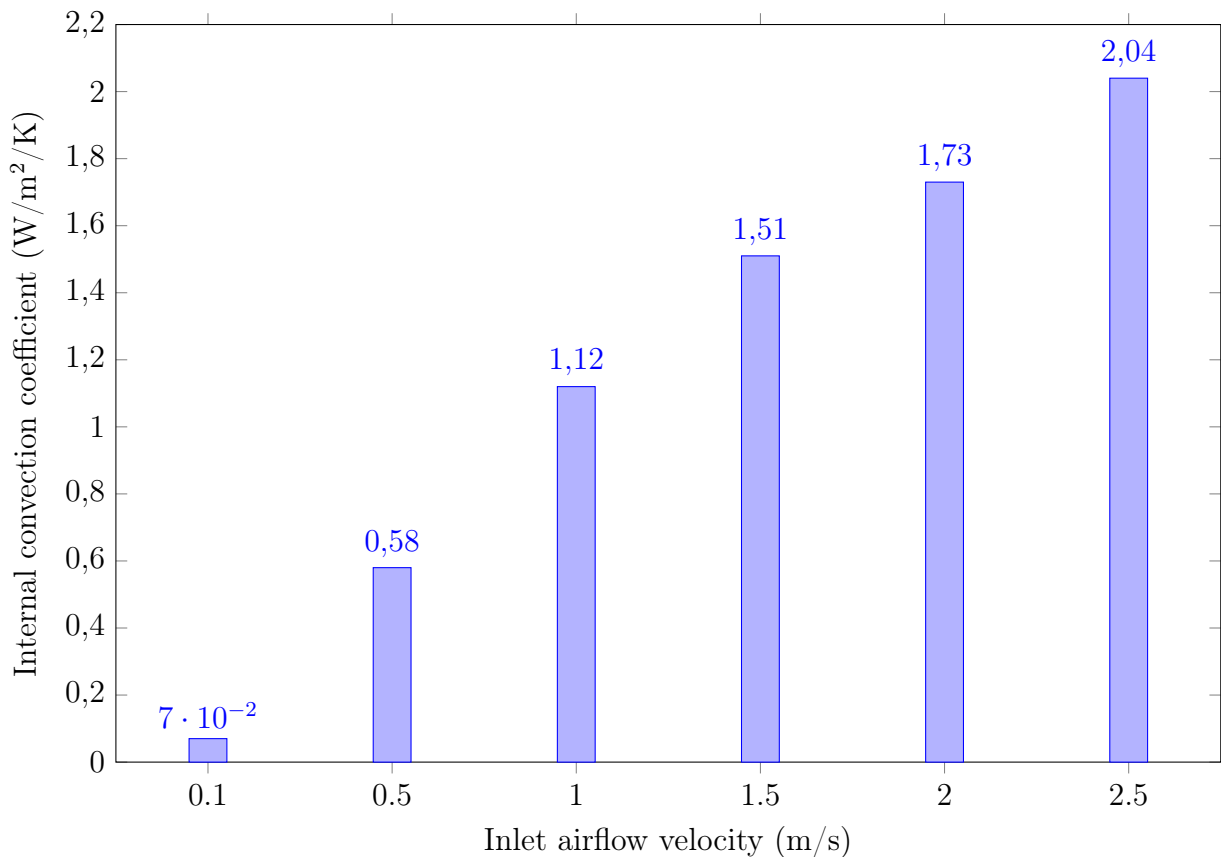


Figure 4.4: Graph : Internal convective heat transfer coefficient on the absorber depending on the velocity - Tilted passive solar dryer model

the external convective coefficient goes from 5 to 30 W/m<sup>2</sup> · K.

Although the external convective heat transfer coefficient has an influence on the solar dryer performances, it also depends on ambient conditions (ambient temperature and wind) and cannot easily be influenced by the design of the solar dryer.

### 4.2.3 Internal convective heat transfer coefficient

The internal convective heat transfer coefficient on the absorber has a major influence on the outlet air temperature, the relative humidity and the outlet absorber temperature. When increasing the internal convective heat transfer coefficient on the absorber, the air at the outlet is at a higher temperature as it can be seen on Figure 4.5. For a constant velocity, increasing the internal convection coefficient on the absorber results in a lower relative humidity for the outlet air. In practice, increasing the convection on the absorber can be done by using fans and in this case, the heat transfer is done by forced convection

between the absorber and the heated air.

The model gives relatively high temperatures for the outlet air compared to the measurements around 57-59 °C (Table 4.5), partly because the internal convective coefficient values are high too. However, the global trend of evolution can be considered as right.

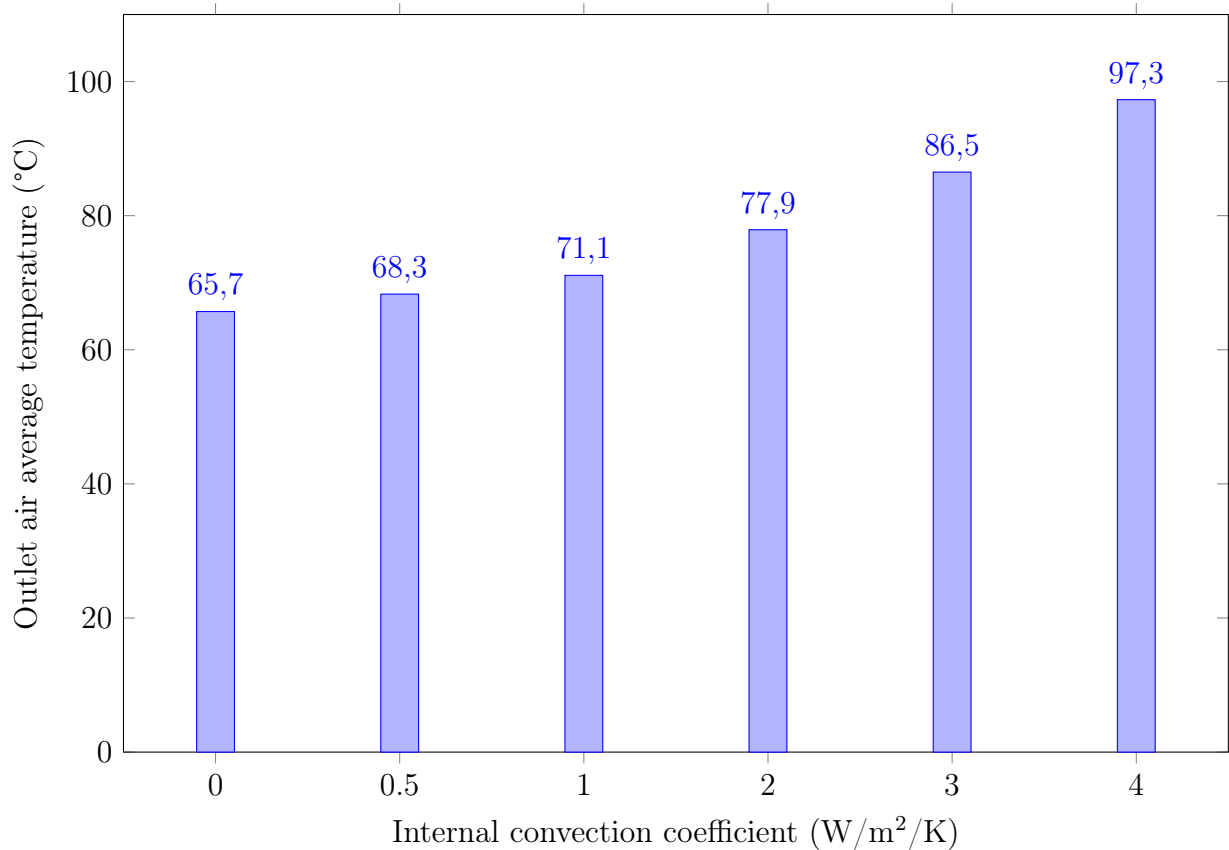


Figure 4.5: Graph - Internal convective coefficient on the absorber plate - Tilted passive solar dryer model

#### 4.2.4 Radiative properties

**Plastic transparency and absorber absorptance** The higher the plastic transparency is, the higher the outlet air temperature will be. Indeed, it means that more solar radiation can be transmitted to the absorber. Since more visible radiation is absorbed by the absorber, it will be able to emit more radiation and thus, heat the air. As shown on Figure 4.6, the transparency of the plastic sheet should be above at least 0,5 so the outlet air temperature is over 50 °C.



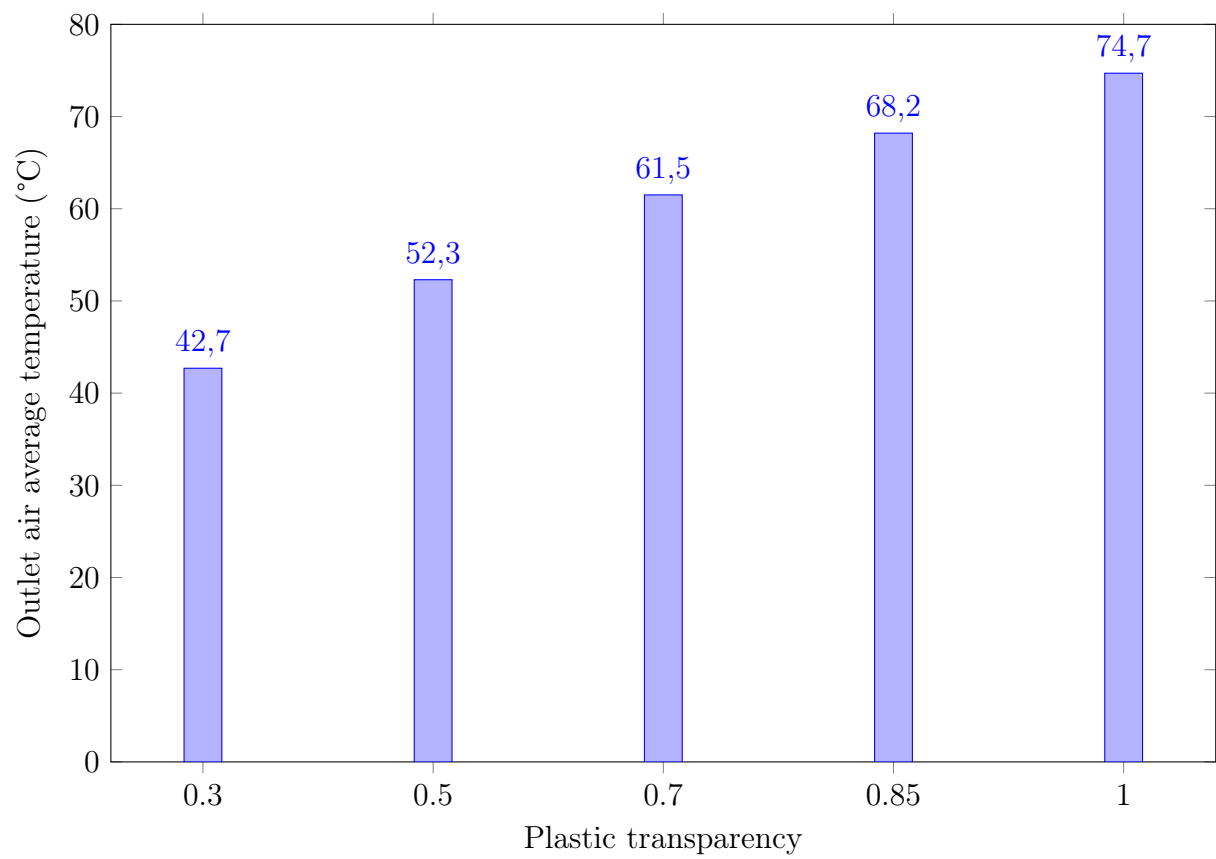


Figure 4.6: Graph - Outlet air temperature and relative humidity depending on the plastic value for transparency

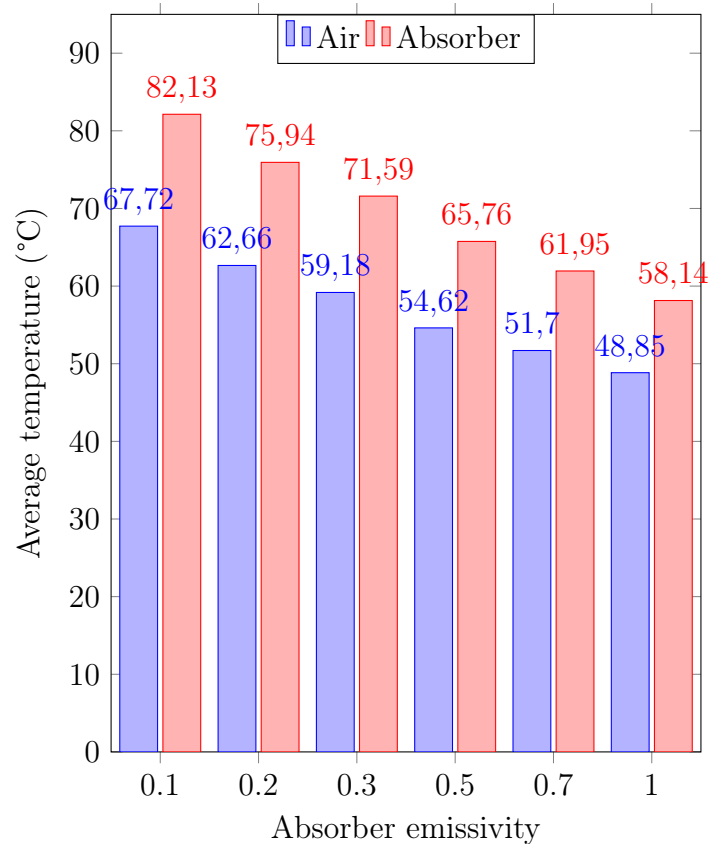


Figure 4.7: Graph - Outlet air and absorber temperature depending on the absorber emissivity

The same trend is observed when changing the absorber absorptance. Looking at the equation 3.6, the absorber absorptance and the plastic transparency play the same role in the calculation of the solar radiation received by the absorber. The best is thus to increase both values in order to get more visible radiation going from the sun to the absorber.

**Absorber emissivity** Simulations were run with the following values for the absorber emissivity : 0,1 ; 0,3 ; 0,5 ; 0,7 ; 1. The value of 1 corresponds to an ideal black body.

The lower the emissivity, the higher the absorber temperature will be and thus the higher the air will be. A low emissivity means that the absorber is losing less heat by radiation since it emits less thermal radiation (visible and infrared). This parameter is material-dependent. Figure 4.7 shows the air and absorber temperatures for the different values of the absorber emissivity.

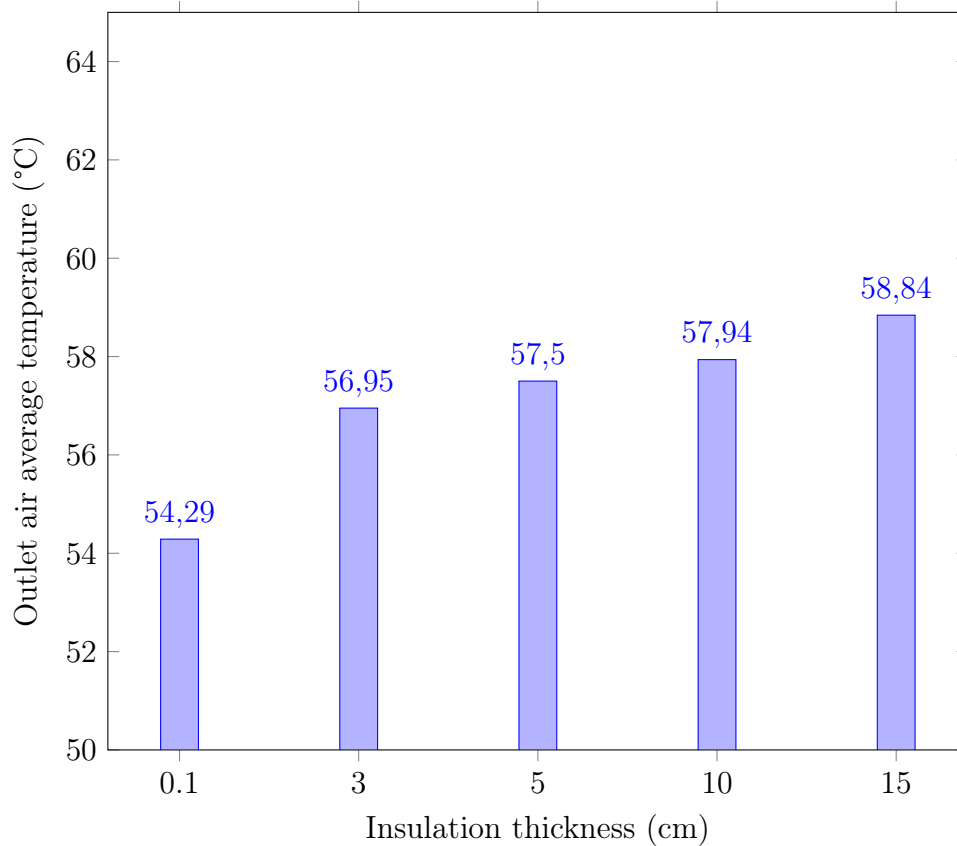


Figure 4.8: Graph - Evolution of the outlet air temperature depending on the insulation thickness

#### 4.2.5 Insulation thickness

The insulation thickness values tested are : 0.1 cm, 1 cm, 3 cm, 5 cm, 10 cm, 15 cm, 20 cm.

Increasing the insulation thickness allows to get higher outlet air temperature to a certain point. After 15 cm, the gain in the outlet air temperature is less perceptible. The same trend is observed with the relative humidity which is slightly lower for a 15 cm insulation thickness (11,9 % compared to 12,6 % for a 3 cm insulation thickness and 12,1 % for 20 cm).

The temperature of the bottom part of the solar dryer is highly impacted by the insulation thickness. The difference between using 1 cm thickness and 10 cm results in a drop in the bottom part temperature from 68,0 °C to 35,1 °C, which means that this temperature is almost divided by 2. However, the difference between 10 cm and 20 cm thickness only implies a drop of the bottom part temperature by 2,3 °C.

### 4.3 Modeling of the active flat solar dryer with SAP-pouches

The active solar dryer uses fans to ensure a better drying of the SAP-pouches. It would be time consuming to model the fans. However, it is possible to increase the airflow velocity inside the solar dryer in the model and this is the solution which has been chosen. The active solar dryer geometry is almost the same as the passive tilted dryer, except that the active solar dryer is flat. Since the pouches are put in the solar dryer on the absorber, this active solar dryer is also direct. The aim of this section is to describe the airflow characteristics in such a dryer with 4 SAP pouches.

#### 4.3.1 Initial values

The input data for this model is the same as for Model 1 (Section 4.1). Only the airflow velocity is changed and increased to 1 m/s to model the fans. This value was measured in the active solar dryer.

#### 4.3.2 Temperature distribution

The model gives temperatures for the different elements of the solar dryer. These temperatures in Table 4.6 are taken at the middle of the solar dryer ( $x = l/2$ ).

Element	Plastic sheet	Air ( $t_{\text{gap}}/2$ )	Absorber	Insulation (2,5 cm)	Bottom
Temperature (°C) outlet surface	28,0	43,2	54,5	45,0	35,9

Table 4.6: Temperatures of the different elements on the front side of the collector

The temperatures are lower in the active dryer than in the passive. This is due to the increased airflow velocity and circulation. Even if the air temperature is lower than in a passive dryer, the higher convection on the SAP-pouches allows a better drying in reality. Also, the bags are directly put on the absorber and receive solar radiation. The air temperature does not reach 50 °C which does not allow the bags to safely dry.

### 4.3.3 Relative humidity

The relative humidity in the active dryer is higher than in the passive one. This is due to the fact that the air can't escape the active dryer since the plastic sheet closes the dryer at the outlet face, only the inlet side is open. The relative humidity is maximal close to the plastic sheet and on the sides of the solar dryer. As well, the relative humidity increases around the bags which are drying (Figure 4.10).

Figure 4.9 shows the relative humidity distribution on the solar dryer. The relative humidity is higher on the sides of the collector and on the plastic sheet. This is characterized by water droplets observed on the active solar dryer.

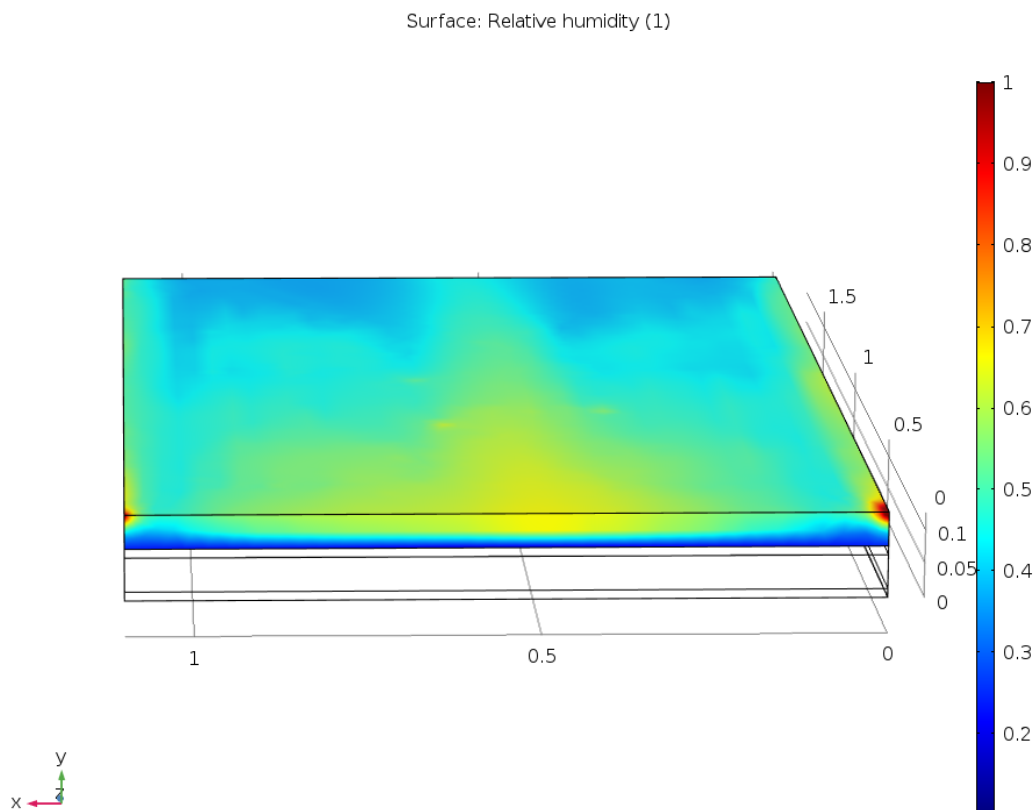


Figure 4.9: Relative humidity distribution around the active solar dryer - Model 2

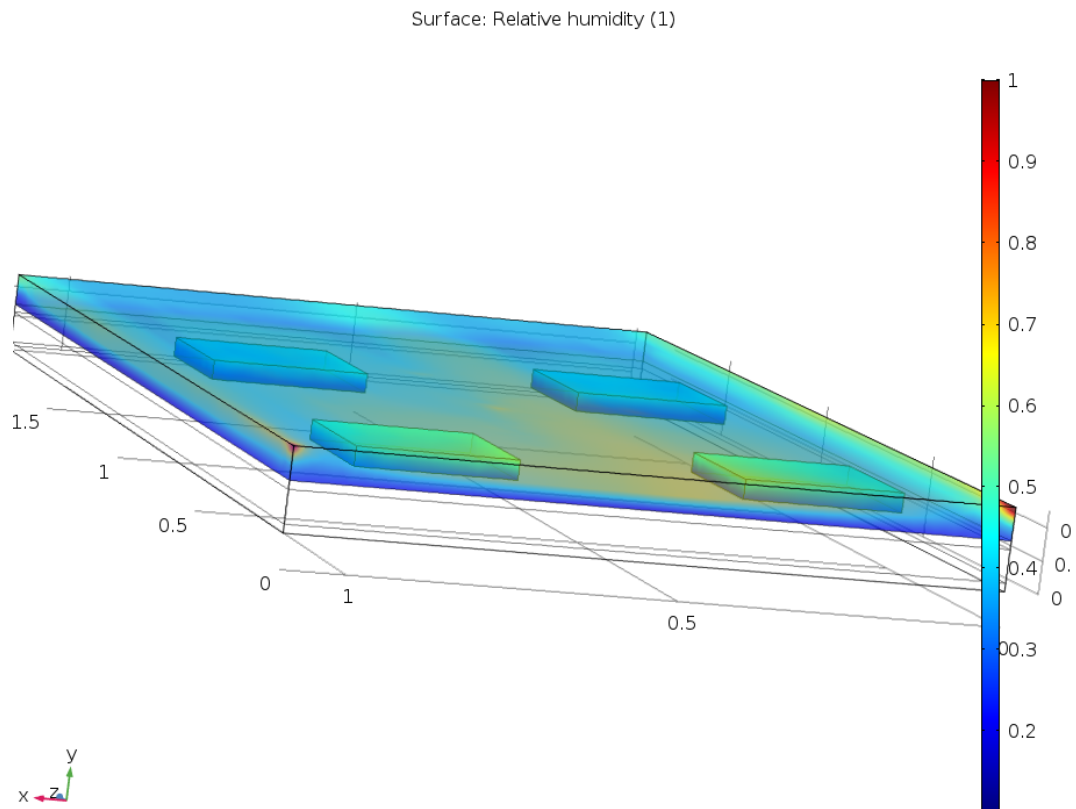


Figure 4.10: Relative humidity distribution inside the active solar dryer - Model 2

#### 4.3.4 Comparison with measurements

Once again, it is possible to compare the calculations done by the model with actual measurements done on the active solar dryer, in Inharrime (June 13th, 2017). The relative error is also calculated, as given in Table 4.7.

The plastic sheet temperature is underestimated by the model. However, the estimation for the insulation temperature, the bottom part and the air in the middle of the solar dryer is under 15 %. The absorber temperature is a bit overestimated but the relative error is still reasonable for the absorber temperature forecast. The global estimation of the model can be considered as good.

The relative humidity in the middle of the solar dryer is about 20 % when measured on-site, in Inharrime. The model forecasts a relative humidity of 18 %. The relative error is about 10 % in this case and it is possible to say that the relative humidity is quite well calculated by the model.

Point #	Component	Measurement	Model 2	Relative error
1	Plastic sheet (L)	41,0 °C	28,6 °C	30,2 %
2	Plastic sheet (C)	41,9 °C	27,0 °C	33,2 %
3	Plastic sheet (R)	39,3 °C	27,8 °C	29,3 %
4	Air (L)	50 °C	42,8 °C	16,8 %
5	Air (C)	46,3 °C	43,2 °C	7,18 %
6	Air (R)	49,7 °C	42,6 °C	14,9 %
7	Absorber (L)	40,6 °C	50 °C	18,8 %
8	Absorber (C)	48,3 °C	54,5 °C	12,8 %
9	Absorber (R)	42,0 °C	48,2 °C	14,8 %
10	Insulation (L)	43,1 °C	42,3 °C	1,86 %
11	Insulation (C)	46,2 °C	45,0 °C	2,67 %
12	Insulation (R)	45,3 °C	42,0 °C	7,28 %
13	Bottom (L)	39,6 °C	34,4 °C	13,1 %
14	Bottom (C)	36,9 °C	35,9 °C	2,71 %
15	Bottom (R)	37,0 °C	34,0 °C	7,03 %

Table 4.7: Comparison between model 1 and actual measurements for temperature





# Chapter 5

## Discussion

### 5.1 Comparison with measurements

When comparing on-site measurements with the modeling simulations, there are several sources of errors to take into account. First, the measurements of the ambient conditions have been done during 3 hours and an average of these conditions was taken whereas the measurements done with the sensors have been run for 30 minutes. The temperatures and relative humidity rates measured in the solar dryer cannot be related to the exact ambient conditions at the time the measure was done. However, this should not be an error of major influence.

The measurement results are subjected to the error resulting from the measurement tool in itself. Then, the placement of the sensor is not as precise as wanted especially for the air temperature measurement. It can explain why the model seems to struggle with giving a good estimate of the temperature on the sides of the passive collector. Finally, the modeling work includes calculation with finite elements. The mesh-dependency has not been studied and there is always a residual error in the calculation.

Of course, a model cannot account entirely for the physical reality of what it aims to model. Hypothesis <sup>1</sup> have been done to simplify the problem and some physical phenomena are harder to model than other (radiation and intern convection for instance). In particular, convection between the air and the topside of the absorber, the inner plastic sides and the downside of the plastic sheet has been modeled by calculating a Nusselt number and then a convective heat transfer coefficient. However, the Nusselt number is determined by empirical correlations as it will be explained in Section 5.2.

The relative error calculated between the measurements and the results from COMSOL

---

<sup>1</sup>mostly hypothesis 3, 5, 6, 8

models should be treated cautiously. The model gives a good overview of the temperatures except for the plastic sheet and the most important is that the air temperature and the relative humidity are quite well predicted with a relative error below 15%. On top of this, the relative errors have been calculated based on the measurements done in Celsius and on the prediction by the model in Celsius as well. Of course, when taking the temperatures in Kelvin, the relative error would drastically decrease since the temperature would be the same but with a reference in Kelvin (over 300 K in general) instead of Celsius (about 40-50 °C).

**Plastic sheet temperature** In both models (passive tilted and flat active), the plastic sheet temperature is underestimated. As a reminder, the heat transfer phenomena taken into account on this surface are : external convection with the ambient air, radiation to the sky, radiation from the absorber and internal convection with the air circulating in the collector.

The sky temperature is rather low (278,15 K) compared to the plastic sheet temperature (average of 310 K) so the radiative heat flux proportional to the difference of these two temperatures at a power of 4 is high. It means that the plastic sheet radiative losses might be higher than the actual radiative losses in the dryer and this could explain the low temperature computed for the plastic sheet. Another source of error could be a too low convective heat transfer coefficient for the convection on the inner side of the plastic sheet. The air circulating in the solar dryer is at a higher temperature than the plastic sheet and some of the heat should be transferred from the air to the plastic sheet. Either the temperature gradient is too low or the convective heat transfer coefficient. Again, the convective heat transfer coefficient value is discussed in Section 5.2.

**Absorber temperature** One approximation has been done regarding the absorber plate shape. The material used in the solar dryers is a corrugated metal sheet. To simplify the problem, it is modeled as a flat sheet which thickness is equal to half of the height of the bumps of the corrugated metal sheet. This height is shown on Figure 5.1. When measuring the absorber temperature, it is always the temperature at the top of the bumps which is collected. A difference of 2,5 to 4°C is observed between the temperatures on the bumps or the hollows.

**Air temperature** As explained in Section 4.3.2, the air temperature does not reach 50 °C in the active solar dryer containing four SAP-pouches full of water, according to the simulation. To ensure product safety, the product should be boiled after the drying in

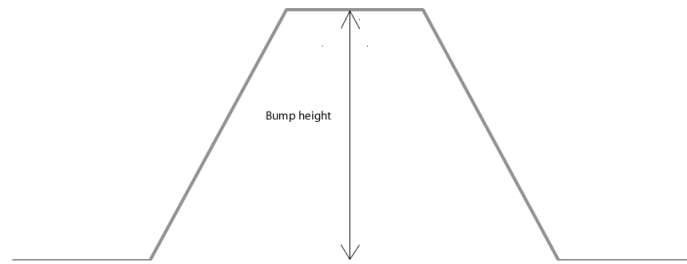


Figure 5.1: Schematics of a bump showing the height of one bump of the metal sheet. This metal sheet is modeled as a flat sheet, which thickness is half of the height of a bump.

the collector. In this case, the product is edible and the product is safe to be stored and consumed later on.

**Insulation temperature** The insulation used to build the solar dryers in Mozambique is a polystyrene slab and insulating expanded foam between this slab and the absorber plate. This material combination doesn't have the same thermal conductivity as rock-wool. To simplify, the insulation conductivity used in the model is the average between the expanded foam conductivity and the polystyrene conductivity. It has an impact on the general performances of the solar dryer and rock-wool or other insulation material with a low thermal conductivity has to be privileged when possible.

## 5.2 Convective coefficient

**External convective coefficient** The external convective coefficient value can either be chosen by the user or computed directly by COMSOL Multiphysics. The two solutions have been tried. The coefficient is calculated by the software according to the formulas given in Section 3.3.3. When using this formulas and for the solar dryer geometry, the convective heat transfer coefficient is about  $2,5 \text{ W/m}^2\cdot\text{K}$ . However, a common value for this coefficient is around  $20 \text{ W/m}^2\cdot\text{K}$  (Olsson 2016). This last value is retained in this work because it seems to be in better agreement with the actual physics of the solar dryer.

The choice of a good value for the external convection coefficient should not be neglected as demonstrated by the parametric studies. It can influence the modeling results with a variation of about  $3\text{-}5 \text{ }^\circ\text{C}$  in the solar dryer components temperatures for an increase of  $5 \text{ W/m}^2\cdot\text{K}$  in the convective coefficient.

**Internal convective coefficient** The internal convection in the solar dryer is one of the most delicate point in this modeling task. With COMSOL Multiphysics, there are several solutions to do so.

One solution is to determine an equivalent conductivity to the convection phenomenon. It is possible to chose the kind of convection which occurs. For the solar dryer, convection in the fluid would occur in the case of an "horizontal cavity heated from below". The software requires to give the dimension of the cavity (distance plastic sheet - absorber) and the temperature difference between the air and the horizontal plate heating the air. This solution might not be the best, first because knowing the temperatures of the air and absorber are one of the goal of the study and are not meant to be set. Also, the software uses some correlations that are not easily accessible.

Another solution is to use another module in the software to model the flow behaviour. Thanks to the Boussinesq approximation for instance, it would be possible to model the natural convection inside a passive solar dryer (Motte, F., Cristofari, C. and Notton, G. 2011). However, in this case, it is time consuming and it could not have been possible to carry out parametric studies with such a model.

Finally, the chosen solution was to calculate the Nusselt number and give it as a parameter in the software. An enhancement of the method proposed by Olsson (2016) is that COMSOL allows to determine the different elements of the Nusselt number formula (specific heat at constant pressure, density, etc) depending on the temperature in each cell of the mesh of the air domain.

- About the friction factor : as written in Section 3.3.3 (Eq. 3.9), the Nusselt number depends on the friction factor. This factor can be calculated as in equation 3.11 (Formula B) or  $f = 0,316Re^{-1/4}$  (Formula A). The graph on Figure 6.1 in Appendix A shows that for a given geometry of the solar dryer and a constant density for air, the two formulas give close values for the convective heat transfer coefficient for airflow velocities between 0,2 m/s and 2,0 m/s. The formula given by equation 3.11 has been arbitrarily chosen.
- About the correlation for the Nusselt number. Once again, several correlations are available to calculate the Nusselt number. The airflow velocity is above 0,5 m/s in the entire work and given the air properties and the geometry of the solar dryers, the Reynolds number for the airflow is always above 10 000. The Prandtl air number is above 0,6 as well given the air properties <sup>2</sup>. In this case, two formulas can be used to calculate the Nusselt number. In the following, Formula C is the formula given

---

<sup>2</sup>see air properties from -150°C to 400 °C - online [http://www.engineeringtoolbox.com/air-properties-d\\_156.html](http://www.engineeringtoolbox.com/air-properties-d_156.html)

by equation 3.9 and Formula D is :  $Nu_D = 0,023Re_D^{4/5}Pr^{0,4}$  (Incropera, F.P. and Dewitt, D.P. 2002). As shown on Figure 6.2 in Appendix A, for Reynolds number between 3000 and 10 000, the two formulas are really close. Then, Formula D gives a higher estimation for the Nusselt number. However, Formula C has been used in the whole simulations, to ensure the continuity with the work done in (Olsson 2016).

## 5.3 Flow modeling

It could have been possible to model the airflow using the Navier-Stokes equations in the Non-Isothermal Flow Module available in COMSOL. However, this method is time-consuming, even using simplifications such as symmetry in the geometry. Some models have been built taking into account the fluid behavior. The results for the temperature and the relative humidity were close to the results given by the model not including the fluid behavior modeling.

Of course, modeling the fluid behaviour gives access to more knowledge about the solar dryer physics. It allows to know the velocity magnitude everywhere in the solar dryer. Normally, it is also possible to model the natural convection in the passive solar dryer by setting boundary conditions on the inlet airflow surface and the outlet airflow surface. If a velocity is taken as boundary condition for the inlet, a pressure has to be the condition for the outlet. However, attempts so far have not given converging models.

The flow modeling requires too much time and knowledge in comparison with the gain in the modeling precision for this thesis work. However, it could be an interesting work to do in the future.

## 5.4 Design optimization

This section aims to present some optimization that could be done on the solar dryers designs. Most of the proposals apply to both solar dryers

### 5.4.1 Solar dryer dimensions

As seen in the parametric studies, the dimension of the gap between the plastic sheet and the absorber can be reduced to a certain point to ensure a higher air temperature in the passive solar dryer and thus a better drying. In practice, this distance is not constant and difficult to control. The plastic sheet tends to bend a little but an average distance between the plastic sheet and the absorber can still be set.

Moreover, the insulation thickness needs to be chosen carefully. A too thick insulation layer is not useful but 5 cm seems to be a minimum value to limit the heat losses and keep the bottom part of the solar dryers at a reasonable temperature. Increasing the thickness of the insulation layer also increases the absorber temperature and in this case, even if more heat is transferred by convection to the air, the temperature difference between the absorber and the plastic sheet is higher and so are the radiative losses from the absorber to the plastic sheet. Finding the minimum thickness needed for the insulation layer allows also to reduce the price of the material needed.

### 5.4.2 Materials' radiative properties

The absorber material should be chosen carefully with the highest absorptance possible and the lowest emissivity. For this, low emitting coating absorbers would of course provide better drying performances. However, the quite high emittance of the absorber (0,8) used to build the solar dryers is sufficient to ensure an air temperature between 50°C and 65 °C and thus food safety regarding the drying product. Since the solar dryers will be built and used in Mozambique, the emittance of the absorber is not a prior concern given the price difference between a classic corrugated metal sheet and a low-emitting coating.

The plastic sheet material choice could be improved by choosing a more transparent material to increase the fraction of solar radiation transmitted to the absorber.

### 5.4.3 Improving convective effects

**On the absorber plate** The aim of the solar dryer is to dry the SAP pouches by creating a low relative humidity. The way of doing it in this work is to increase the air temperature and have it circulating around the bags. Increasing the convection on the absorber plate is a way of transferring more heat to the air. One way of increasing this convection is to increase the surface of contact between the air and the absorber.

In the passive solar dryer, only natural convection occurs. To increase the heat transfer from the absorber to the air, an easy solution is to increase the absorber temperature by choosing better materials or a better orientation of the solar dryer toward the sun. Then the temperature difference between the inlet air and the absorber higher and so is the heat transfer. Then, a better way of increasing the convective heat transfer is to increase the convective heat transfer coefficient, which means increasing the Nusselt number or the hydraulic diameter (the effective surface of the absorber). It could be possible to increase the natural convection thanks to a double-pass system with the air entering on the backside of the passive solar dryer and then going around the absorber plate and exiting the solar

dryer on the opposite side to the one the air entered. In the active solar dryer, forced convection occurs. In this project, fans were used to ensure a higher airflow velocity.

**Around the bags** The convection around the bags is also very important. As explained in (Phinney and Tivana 2016), the higher the airflow velocity around the bags, the higher the drying rate. One idea to increase the amount of air passing around the bags could be to have air passing above and under the bags. In the passive solar dryer, the bags should be put higher in the drying chamber joined to the collector. However, a balance has to be found because the driest air is located close to the absorber plate. In the active solar dryer, the fans already provide a good circulation of air around the bags. The point in this is also to avoid the moisture to stay on the bag so the relative humidity does not increase too consequently around the bags.

#### 5.4.4 Balance airflow velocity / relative humidity / convection

When increasing the airflow velocity and circulation in a solar dryer thanks to fans for instance, the convection effect around the bags increases. According to (Phinney and Tivana 2016), the wind around the bags is necessary to enhance the drying process. On the other hand, increasing the airflow velocity let less time for the absorber to heat the passing air. With an airflow of 1,5 m/s and a collector length of 1,8 m, an air molecule would stay 1,2 s in the dryer. Also, a higher velocity is responsible for a lower air temperature in the dryer and a higher relative humidity (Section 4.2.1). This means that a balance between the airflow, the temperature and the relative humidity has to be done to ensure a sufficiently high temperature (above 50 °C), a relatively low relative humidity (under 15-20 %) and enough convective effects around the bags (airflow velocity around 1 m/s).





# Conclusion

The models created in COMSOL Multiphysics give sufficient information regarding the temperatures and air relative humidity in several parts of both a direct and indirect solar dryer. Even if the exact temperatures might not be found, the models give correct approximation of it. The main purpose of these models is to study the effect of different parameters variation. The main conclusions of this work are :

- COMSOL is a sufficient tool to build models. It will also allow to improve the modeling by including more phenomena (water vapor transport for instance).
- The models gives a sufficient estimation of the temperature and relative humidity in a direct and in an indirect solar dryer with a maximum error of 30 %.
- The calculations of the external convective coefficient can be done with different formulas without changing the results in a significant way. However, the calculation of the internal convective coefficient is more important and the formula used to calculate requires to be chosen carefully depending on the flow characteristics (Reynolds number, Prandtl number).
- It is possible to increase the performance of the two solar dryers tested by reducing the space between the absorber and the plastic sheet and by using an insulation layer of at least 5 cm.
- The choice of a low-emissivity material for the absorber is not of prime importance. However, the plastic sheet could be of higher quality with a higher transparency.
- A balance has to be found between the airflow velocity, the relative humidity and the convection provided on the absorber plate and around the bags.



# Recommendations for future work

The modeling work could be improved by :

- Making more measurements on the actual solar dryers varying the weather condition (temperature, relative humidity, irradiation) to study the influence of the weather on the dryers' performances.
- Modeling the drying process using mass and heat transfer theory in COMSOL Multiphysics using the Transport of Diluted Species and Heat Transfer module to obtain more precised calculations in modeling the solar dryers with SAP pouches inside.
- Measuring the convective heat transfer coefficient. The internal convection coefficient used in the models are highly unprecise but have a major influence on the air temperature calculations.
- Simulating the sun as an external source of power instead of applying a boundary heat source on the absorber. By setting the material properties (emissivity, absorptance) depending on the wavelength of the radiation, it is possible to calculate the surface-to-surface radiation exchange in the solar dryer with COMSOL Multiphysics.
- Creating a time-dependent model based on weather date (provided by COMSOL or downloaded by the user).
- Creating a COMSOL application which facilitates the parametric studies. The user changes the parameters and the calculations are automatically launched.
- Combining this work with the models of the SAP pouches which will be soon done by Randi Phinney as part of her PhD thesis.



# Chapter 6

## Appendix

### A Friction factor and Nusselt number

The two graphs used to compared respectively Formulas A and B and C and D are presented below on Figure 6.1 and 6.2.

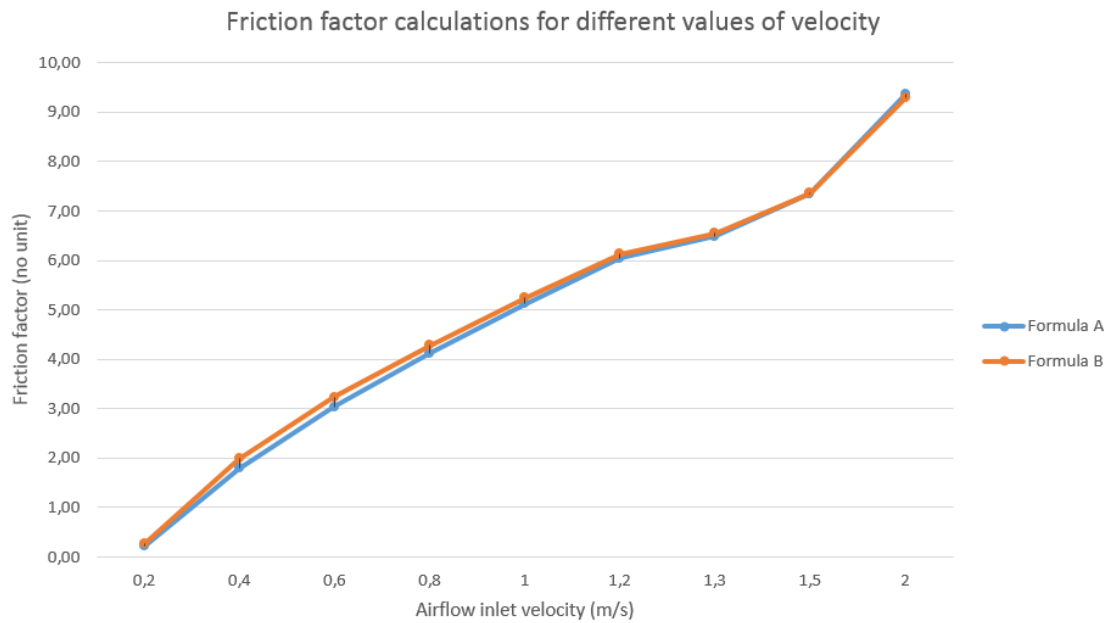


Figure 6.1: Graph : Friction factor for different values of airflow velocity - comparison of two formulas

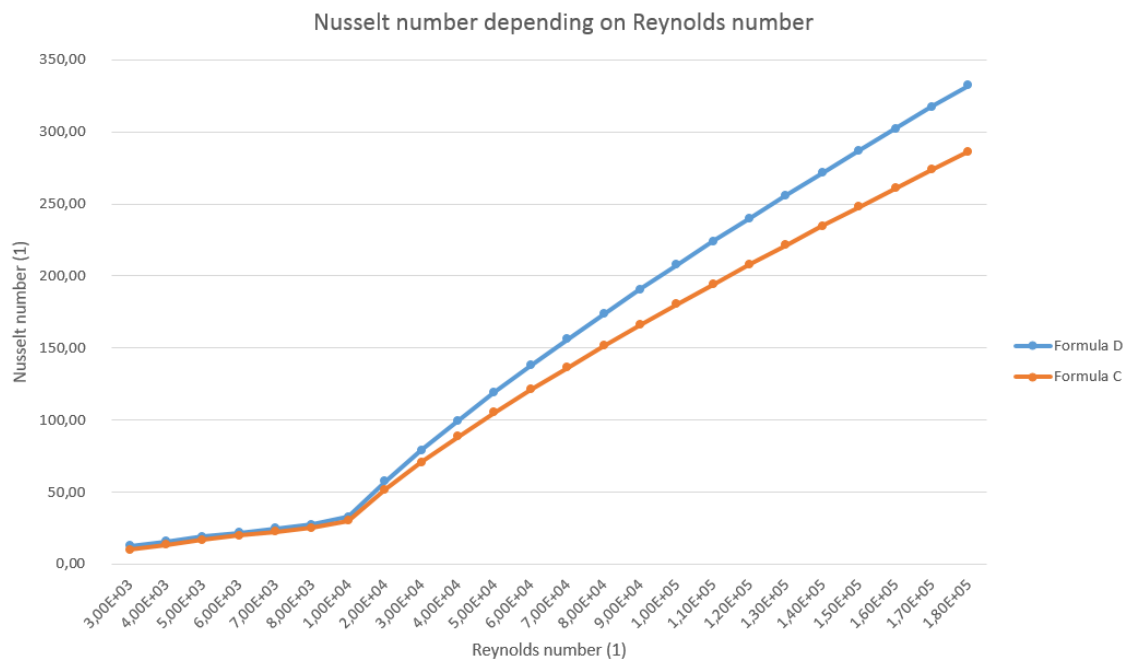


Figure 6.2: Graph : Nusselt number for different values of airflow velocity - comparison of two formulas

# Bibliography

- Amin, A. Z. (2013). *Mozambique Renewable Readiness Assessment 2012*. Ed. by IRENA, p.15.
- Andersson, L. (2016). “Combining Solar Thermal and Membrane Technologies”. Unpublished. Master thesis. Lund University.
- Augustus, L., Kumar, S. and Bhattacharya, S.C. (2002). “A comprehensive procedure for performance evaluation of solar food dryers”. In: *Renewable and Sustainable Energy Reviews* 6, pp. 367–393.
- Bengtsson, G. and Döhlen, V. (2016). “Performance testing of a Solar Thermal Fruit Dryer”. Master thesis. Lund University: Faculty of Engineering, Lund University, Lund.
- Cengel, Y., Cimbala, J. and Turner, R. (2012). *Thermal-fluid Sciences*. Ed. by McGrawHill. 4th. Chap. 21, p. 887.
- Centrale Intelligence Agency (2007). *The World Factbook*. Chap. Mozambique. URL: <https://www.cia.gov/library/publications/the-world-factbook/geos/mz.html>.
- Ekechukwu, O.V. and Norton, B. (1999). “Review of solar-energy drying systems II : an overview of solar drying technology”. In: *Energy Conversion Management* 40, pp. 615–655.
- Food Agricultural Organization of the United Nations, ed. (2014a). *Crops Production*. URL: <http://www.fao.org/faostat/en/#compare>.
- ed. (2014b). *Food Balance*. URL: <http://www.fao.org/faostat/en/#compare>.
- (2016). *Evolution of the number of people undernourished (1990-2015)*.
- Hammar, L. (2011). *Distribution of Wind and Solar Energy Resources in Tanzania and Mozambique*, p.8. URL: [http://publications.lib.chalmers.se/records/fulltext/local\\_150046.pdf](http://publications.lib.chalmers.se/records/fulltext/local_150046.pdf).
- Hegde, V.N., Hosur, V.S., Rathod, S.K., Harsoor, P.A. and Narayana, K.B. (2015). “Design, fabrication and performance evaluation of solar dryer for banana”. In: *Energy, Sustainability and Society* 5.1, p. 23. ISSN: 2192-0567. DOI: 10.1186/s13705-015-0052-x. URL: <http://dx.doi.org/10.1186/s13705-015-0052-x>.

- Incropera, F.P. and Dewitt, D.P. (2002). *Fundamentals of heat and mass transfer*. English. Ed. by New York : Wiley. 5th.
- Instituto Nacional de Estatística (2012). *Moçambique Inquérito Demográfico e de Saúde 2011*.
- Kumar, M. (2010). *Pervaporation : an overview*. URL: <http://www.cheresources.com/content/articles/separation-technology/pervaporation-an-overiew?pg=2>.
- Kumar, M., Sansaniwal, S.K. and Khatak, P. (2016). “Progress in solar dryers for drying various commodities”. In: *Renewable and Sustainable Energy Reviews* 55, pp. 346–360.
- Motte, F., Cristofari, C. and Notton, G. (2011). “Thermal Modeling of a Solar Water Collector Highly Building Integrated”. In: [Accessed 23/05/2017]. Proceedings of the 2011 COMSOL conference. Stuttgart. URL: [https://www.researchgate.net/profile/G\\_Notton/publication/266412238\\_Thermal\\_Modeling\\_of\\_a\\_Solar\\_Water\\_Collector\\_Highly\\_Building\\_Integrated/links/55293d530cf2779ab79077be/Thermal-Modeling-of-a-Solar-Water-Collector-Highly-Building-Integrated.pdf](https://www.researchgate.net/profile/G_Notton/publication/266412238_Thermal_Modeling_of_a_Solar_Water_Collector_Highly_Building_Integrated/links/55293d530cf2779ab79077be/Thermal-Modeling-of-a-Solar-Water-Collector-Highly-Building-Integrated.pdf).
- Multiphysics, COMSOL (2012). *Heat transfer module user’s guide*. URL: <http://www.ewp.rpi.edu/hartford/~collir5/MP/OTHER/Reference/HeatTransferModuleUsersGuide.pdf>.
- Olsson, J. (2016). “Modelling of a solar dryer for fruit preservation in developing countries”. Master thesis. Lund University: Faculty of Engineering, Lund University, Lund.
- Onwunde, D. I., Norhashila, H. , Rimfiel, B.J., Nazmi, M.N. and Khalina, A. (2010). “Modeling the Thin-Layer Drying of Fruits and Vegetables : A review”. In: *Comprehensive Reviews in Food Science and Food safety* 15, pp. 599–618.
- Phinney R., Rayner M. and L. Tivana (2016). “Solar Assisted Pervaporation (SAP) for Preserving and Utilizing Fruits in Developing Countries”. In:
- Phinney, R., Rayner, M., Sjöholm, I., Tivana, L. and Dejmek, P. (2015). “Solar Assisted pervaporation (SAP) for preserving and utilizing fruits in developing countries”. In: Third Southern African Solar Energy Conference. South Africa.
- Sharma, A., Chen, C.R. and Vu Lan, N. (2009). “Solar-drying systems : a review”. In: *Renewable and Sustainable Energy Reviews* 13, pp. 1185–1210.
- Singh Chauhan, P., Kumar, A. and Tekasakul, P. (2015). *Applications of software in solar drying systems: A review*. URL: [https://www.researchgate.net/publication/291808090\\_Applications\\_of\\_software\\_in\\_solar\\_drying\\_systems\\_A\\_review](https://www.researchgate.net/publication/291808090_Applications_of_software_in_solar_drying_systems_A_review) (visited on 04/28/2017).
- Singh, P. and Heldman, D.R. (2013). *Introduction to Food Engineering*. Ed. by S.L. Taylor. 4th edition. Food Science and Technology, International Series. Elsevier. Chap. 12.



- SIPER (2011). *Rockwool technical insulation data sheet*. [Accessed : 28/04/2017]. URL: [http://www.siper-bg.com/files/products/pic136\\\_1\\\_en.pdf](http://www.siper-bg.com/files/products/pic136\_1\_en.pdf).
- TataSteel (2014). *ColorCoat HPS200 Ultra Technical details*. [Accessed : 28/04/2017]. URL: [https://www.tatasteelconstruction.com/static\\_files/Tata%20Steel/content/products/Colorcoat/Colorcoat%20HPS200%20Ultra/EN%20UK/New%20Downloads/Colorcoat%20HPS200%20Ultra%20C2%AE%20technical%20manual.pdf](https://www.tatasteelconstruction.com/static_files/Tata%20Steel/content/products/Colorcoat/Colorcoat%20HPS200%20Ultra/EN%20UK/New%20Downloads/Colorcoat%20HPS200%20Ultra%20C2%AE%20technical%20manual.pdf).
- TechnoServe (2002). *Briefing Document The Mozambican Fruit Industry*. URL: <http://www.speed-program.com/wp-content/uploads/2012/09/Fruit-Briefing-Document-TechnoServe-2002.pdf>.
- VijayaVinkataRaman, S., Iniyar, S. and Goic, R. (2012). "A review of solar drying technologies". In: *Renewable and Sustainable Energy* 16, pp. 2652–2670.

This degree project for the degree of Master of Science in Engineering has been conducted at the Division of Heat Transfer , Department of Energy Sciences, Faculty of Engineering, Lund University.

Supervisor at the Division of Heat Transfer was Dr. Martin Andersson  
Supervisor at Department of Energy and Building Design was Henrik Davidsson  
Examiner at Lund University was Professor Bengt Sundén

The project was carried out in cooperation with the Department of Food Technology at Lund University and University Eduardo Mondlane, Mozambique.

Thesis for the Degree of Master of Science in Engineering

ISRN LUTMDN/TMHP-17/5385-SE

ISSN 0282-1990

© 2017 Juliette Chaignon samt Energy Sciences

Efficient Energy Systems

Department of Energy Sciences

Faculty of Engineering, Lund University

Box 118, 221 00 Lund

Sweden

[www.energy.lth.se](http://www.energy.lth.se)